



**PRELIMINARY MAGNETIC DESIGNS
FOR LARGE-BORE AND HIGH-FIELD DIPOLE MAGNETS***

D. Leroy¹ and O. Vincent-Viry²

This report presents the results of calculations - magnetic, forces, conductor losses - for dipole magnets having bores of 88, 130, 160 mm. The calculations are made for two types of dipole design: a layer design and a slot design. The aim of these calculations was to define the characteristics of a Nb₃Sn strand suitable to reach dipolar field in the range 13 to 15 T. This report constitutes a deliverable for the NED Joint Research Activity within the CARE Program.

¹ CERN, Accelerator Technology Department, Geneva, Switzerland

² Formerly CERN, Accelerator Technology Department, Geneva, Switzerland

Departmental Report

CERN/AT 2004-22 (MAS)
NED

**PRELIMINARY MAGNETIC DESIGNS
FOR LARGE-BORE AND HIGH-FIELD DIPOLE MAGNETS***

D. Leroy¹ and O. Vincent-Viry²

This report presents the results of calculations - magnetic, forces, conductor losses - for dipole magnets having bores of 88, 130, 160 mm. The calculations are made for two types of dipole design: a layer design and a slot design. The aim of these calculations was to define the characteristics of a Nb₃Sn strand suitable to reach dipolar field in the range 13 to 15 T. This report constitutes a deliverable for the NED Joint Research Activity within the CARE Program.

1 CERN, Accelerator Technology Department, Geneva, Switzerland

2 Formerly CERN, Accelerator Technology Department, Geneva, Switzerland

*This work was supported in part by the European Community-Research Infrastructure Activity under the FP6 "Structuring the European Research Area" program (CARE, contract number RII3-CT-2003-506395)

Administrative Secretariat
AT Department
CERN
CH - 1211 Geneva 23

Geneva, Switzerland
December 2004

Table of contents

1. INTRODUCTION	1
2. GENERALITIES ON STRAND, CABLE AND MAGNET STRUCTURE	2
3. LAYER DESIGN	5
3.1 Magnet general layout of a 88mm bore dipole	5
3.2 Cable configurations	5
3.3 Impact of various parameters: the cable strand number, strand diameter, copper to non copper ratio	6
3.3.1 Impact of strand number and strand diameter	6
3.3.2 Impact of strand diameter	7
3.3.3 Impact of strand number in cable	8
3.3.4 Impact of Cu/non Cu ratio	8
3.3.5 Conclusions	8
3.4 Base line design for a two layer, 88 mm bore dipole	9
3.4.1 Magnetic aspects	9
3.4.1.1 Magnetic field distribution	9
3.4.1.2 Peak fields in blocks and load lines	10
3.4.1.3 Magnet transfer function	11
3.4.1.4 Magnetic field leakage	12
3.4.2 Electromagnetic Forces	12
3.4.3 Losses in conductors	13
3.4.3.1 Hysteretic losses	13
3.4.3.2 Inter-filament losses	13
3.4.3.3 Inter-strands coupling losses	14
3.4.4 Overall Characteristics of the 88 mm, two layers, base line design	14
3.4.5 Considerations on the mechanical design	15
3.5 A 88 mm dipole with 2 types of cables	15
3.6 Base line design for a two layers, 130 mm bore dipole	16
3.6.1 Magnetic aspects of a 130 mm layer design dipole	17
3.6.2 Electro-magnetic force aspects of a 130 mm layer design dipole	18
3.6.3 Conductor losses in a 130 mm layer design dipole	18
3.6.3.1 Hysteretic losses	18
3.6.3.2 Inter-filament losses	18
3.6.3.3 Inter-strands coupling losses	19
3.6.4 Overall Characteristics of the 130 mm, two layers, base line design	20
3.7 Base line design for a two layers, 160 mm bore dipole	20
3.7.1 Magnetic aspects of a 160 mm layer design dipole	21
3.7.2 Electro-magnetic force aspects of a 160 mm layer design dipole	22
3.7.3 Conductor losses in a 160 mm layer design dipole	23
3.7.3.1 Hysteretic losses	23
3.7.3.2 Inter-filament losses	23
3.7.3.3 Inter-strands coupling losses	24
3.7.4 Overall Characteristics of the 160 mm, two layers, base line design	24
4. SLOT DESIGN	25
4.1 Magnet general layout	25
4.2 Conventions and naming for the electro-magnetic force calculations	27
4.3 Variations of design parameters for slot magnets	27
4.3.1 Impact of the number of conductors	28

4.3.2	Impact of notch angle and notch length -----	28
4.3.2.1	Variation of the angle of one notch (Annex IV, IV.2.1.) -----	29
4.3.2.2	Variation of the length of one notch (Annex IV, IV.2.2.) -----	29
4.3.3	Impact of notch width -----	30
4.3.4	Impact of notch number -----	30
4.4	Base line design of a slot type dipole of 88 mm aperture -----	30
4.4.1	Magnetic aspects of a 88 mm slot design dipole -----	31
4.4.2	Electro-magnetic forces aspects of a 88 mm slot design dipole -----	32
4.4.3	Conductor Losses of a 88 mm slot design dipole -----	34
4.4.3.1	Hysteretic losses -----	34
4.4.3.2	Inter-filament losses -----	34
4.4.3.3	Inter-strands coupling losses: -----	35
4.4.4	Overall Characteristics of the 88 mm, base line slot design -----	36
4.5	Base line designs for a slot type dipole of 130 mm aperture -----	36
4.5.1	Magnetic aspects of a 130 mm slot design dipole -----	36
4.5.2	Electro-magnetic force aspects of a 130 mm slot design dipole -----	37
4.5.3	Conductor Losses in a 130 mm slot design dipole -----	39
4.5.3.1	Hysteretic losses -----	39
4.5.3.2	Inter-filament losses -----	39
4.5.3.3	Inter-strands coupling losses -----	40
4.5.4	Another design, with larger cable, of a 130 mm slot type dipole -----	40
4.5.5	Comparison of the two 130 mm slot design CRT9 and CRT9_31 -----	44
4.6	Base line designs for a slot type dipole of 160 mm aperture -----	44
4.6.1	Magnetic aspects of a 160 mm slot design dipole -----	45
4.6.2	Electro-magnetic force aspects of a 160 mm slot design dipole -----	45
4.6.3	Conductor Losses in a 160 mm slot design dipole -----	47
4.6.3.1	Hysteretic losses -----	47
4.6.3.2	Inter-filament losses -----	47
4.6.3.3	Inter-strand coupling losses -----	48
4.6.4	Another design, with larger cable, of a 160 mm slot type dipole -----	49
4.6.5	Comparison of the two 160 mm slot design CRT14 and CRT14_31 -----	53
5.	<i>COMPARISON OF SLOT AND LAYER DESIGNS AS A FUNCTION OF APERTURE -----</i>	54
6.	<i>MULTIPOLE OPTIMISATION IN THE SLOT DESIGN -----</i>	56
7.	<i>MULTIPOLE COMPENSATION AT LOW FIELD -----</i>	58
8.	<i>CONCLUSION -----</i>	60
9.	<i>REFERENCES -----</i>	61
10.	<i>ANNEX I -----</i>	63
11.	<i>ANNEX II -----</i>	65
12.	<i>ANNEX III -----</i>	67
13.	<i>ANNEX IV -----</i>	69
14.	<i>ANNEX V -----</i>	74

1. INTRODUCTION

The NED project is one of the Joint Research Activities (JRA) approved by EU in the frame of CARE program [1] in view of developing high field accelerator magnets in Europe.

At the EU's request, the initial NED proposal has been divided into two Phases:

- Phase I covers conductor development and includes some limited studies on conductor insulation (representing about 25% of the initial program)
- Phase II is devoted to the detailed design, manufacturing and test of the dipole magnet model [2].

Six institutes have agreed to collaborate to the NED JRA:

- CCLRC-RAL (United Kingdom)
- CEA/DSM/DAPNIA (France)
- CERN/AT (International)
- INFN – Milano/LASA and Genova (Italy)
- University of Twente (The Netherlands)
- University of Wroclaw (Poland).

Phase I of NED is articulated around three main work packages: (1) Thermal Studies and Quench Protection (TSQP), (2) Conductor Development (CD) and (3) Insulation Development and Implementation (IDI).

The CD work package is coordinated by CERN.

The core of the activity will be devoted to wire and cable development but it includes the preliminary designs of a large-aperture and high-field (up to 15 T) Nb₃Sn dipole magnet in order to derive meaningful conductor specifications: mainly the critical current density in the non-copper part and the strand dimensions.

It was foreseen in the NED proposal to make a review and analysis of the various dipole designs. This work package has been withdrawn in the project re-profiling due to the limited funding. Preliminary magnetic designs for large bore and high - field dipole magnets has been then incorporated in the CD package in order to define the Nb₃Sn strand characteristics suitable for large field applications.

Preliminary studies of the various optical schemes for LHC upgrade have shown the necessity to have dipoles reaching fields larger than 11 T in large bore apertures. Moreover, the magnets will be exposed to high beam losses in their mid-plane.

The preliminary dipole studies have considered the 3 apertures of 88, 130, 160 mm.

To calculate the limits in fields in the magnet, it is necessary to have in mind some initial constrains imposed on the conductor and some views on the magnet mechanical structure.

The critical current density in the non-copper cross-section of the Nb₃Sn strand is assumed to be 1500A/mm² at 15 T and 4.2 K. This high critical current density is considered as the goal of a R&D development program for the strand.

The present study concentrates on two types of magnetic designs: a layer design and a slot design, for which there exists some previous experience of construction for dipole fields up to 10 T.

The aim of the preliminary design studies is not to make a detailed mechanical design of the dipoles but to show the trends and possibilities existing in the two types of designs. The detailed mechanical designs will have to be revisited in the future.

This report presents for each type of magnet configuration -called layer design or slot design- the calculation and distribution of magnetic field and forces, and of the conductor losses, for the 3 apertures of 88, 130, 160 mm.

Each design is treated in a different paragraph.

At the end, we show ways of compensating the harmonics generated by conductor distribution in the slot design and principles of compensation of the harmonics due to the effective larger size of filaments inherent to the Nb₃Sn technology.

This report constitutes a deliverable for the NED Joint Research Activity within the CARE Program.

2. GENERALITIES ON STRAND, CABLE AND MAGNET STRUCTURE

Strands:

The first basic choice concerns the critical current density in the non-copper area for Nb₃Sn strands, which has been fixed as a goal for the conductor development at 1500 A/mm², 4.2 K, in an external field of 15 T.

The second basic choice concerns the copper to non-copper ratio which has been fixed to 1.25 to 1, to have a current density in the copper at quench around 1100 A/mm², values normally used at present in the magnet for their protection in case of quench. It is not excluded that higher current densities in copper could be used following the studies on quench protection and thanks to the high quench velocities measured at high field in the Nb₃Sn magnets.

Cables:

- The maximum strand number is limited to 40 strands, given by the existing cabling machines in Europe.
- There are two types of magnet designs. In both designs, the coil structure has blocks and the current distribution approaches a cos θ type. One approach is based on the layer design and uses a keystone cable. The other, called slot design, uses a rectangular cable.
- A 10% critical current degradation due to cabling has been assumed. It is a reasonable goal. The cable degradation will be measured in the course of the conductor development as well as the pressure effect on the cable characteristics. The keystone cable could have more degradation on the thin edge than the rectangular cable. No supplementary degradation due to transversal pressure effects on cables has been taken into account.

- The electrical insulation is assumed to be 0.2 mm thick on each cable side.
- The geometrical dimensions of cables are determined from the following formulas to ensure a good mechanical stability and less cabling degradation. They are based on the work made at LNBL [3]. In the mentioned reference, there exists more experimental data of the degradation for rectangular cables; the degradation for keystone cables has still to be investigated.

for keystone cable:

$$height = 1.04 \frac{nbr_str}{2} \phi_{str}$$

$$width_inner = 2 * 0.87 \phi_{str} ; width_outer = 2 * 0.95 \phi_{str}$$

where ϕ_{str} is the strand diameter and nbr_str the number of strands in the cable.

for rectangular cable:

$$height = 1.04 \frac{nbr_str}{2} \phi_{str} ; width = 2 * 0.87 \phi_{str}$$

Magnet:

To calculate the magnetic and electrical characteristics, one needs to have in mind a basic conceptual mechanical design. The same approach will be taken for all the comparative studies. The present study has been concentrated on 3 bore diameters: 88, 130, and 160 mm.

- There exists an intermediate spacer (collars) between the coils and the iron in the case of the layer design.
- For the slot design, the conductors are wound in a metallic structure participating in the force transmission.
- The iron yoke is split horizontally to benefit from the iron inertia to sustain the high horizontal forces. The iron thickness is estimated on a criterion of flux return and a mechanical approach to guarantee that the horizontal gap stays closed at high field like it is for MFRESCA [4].
- The coil ends are supposed to be maintained in a cage for the slot design (MFISC Dipole Magnet) [5].
- An outer stainless steel cylinder closes the structure. The thickness of the outer cylinder is estimated to ensure that the horizontal iron gap stays closed in all the magnet operating conditions; its value is then different for each dipole aperture.

Magnetic calculations with finite iron have been carried out by mean of the code ROXIE [6]. For the slot design, it has been necessary to elaborate a tool for the preparation of the block geometry before using ROXIE [7].

Losses in conductor:

The different types of losses occurring in the magnet will be estimated according to the following relations [8]:

Losses due to the magnetization of the filaments:

$$Q_{\text{hyst}} = \oint \frac{2d_f}{3\pi} J_c(B) \cdot \text{sgn}(dB/dt) \cdot dB \quad [\text{J/m}^3/\text{cycle}] \quad (1)$$

d_f : effective filament diameter

Losses due to inter-filaments coupling currents:

$$P_{\text{if}} = \left(\frac{L_{p,f}}{2\pi} \right)^2 \frac{(dB/dt)^2}{\rho_{\text{eff}}} \quad [\text{W/m}^3] \quad (2)$$

$L_{p,f}$: twist pitch of the filaments

ρ_{eff} : matrix effective transverse resistivity

Losses due to inter-strands coupling currents:

$$P_{\text{a}} = 0.17 \frac{L_{p,s} h^2 (1 - 1/N_s)}{R_a} \left(\frac{dB_{\text{per}}}{dt} \right)^2 + 0.125 \frac{L_{p,s} w^2}{R_a} \left(\frac{dB_{\text{par}}}{dt} \right)^2 \quad [\text{W/m}] \quad (3)$$

$$P_{\text{c}} = 8.49 \cdot 10^{-3} \frac{L_{p,s} h^2 (N_s^2 - N_s)}{R_c} \left(\frac{dB_{\text{per}}}{dt} \right)^2 \quad [\text{W/m}] \quad (4)$$

$L_{p,s}$: twist pitch of the strands

h, w : height and mid-width of the cable

R_a : resistance between to adjacent strands

R_c : resistance between crossing strands

B_{par} : field component parallel to the cable height

B_{per} : field component perpendicular to the cable height

3. LAYER DESIGN

3.1 Magnet general layout of a 88mm bore dipole

All the magnet structures, which have been investigated, are based on the same layout of principle.

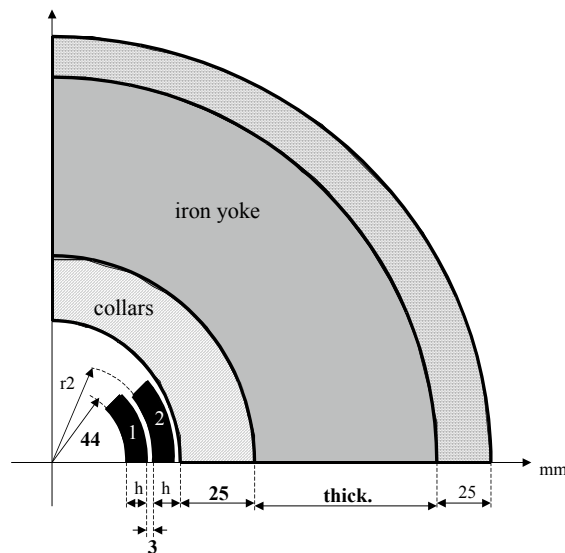


Fig. 1 Magnet cross section (layer design)

The coil radius is 44 mm; there is a 3 mm space between the two layers (wound with the same cable). The iron yoke is separated from the coils by an intermediate spacer (collars) of 25 mm thickness and surrounded by a thick stainless steel shrinking cylinder. In the magnetic calculations, the fringing field have been calculated with a 25 mm outer cylinder. Mechanical estimations have lead to increase the thickness of the outer cylinder to 28 mm.

The inner layer consists of 4 blocks of conductors while the outer is made of 3 blocks. The adjacent blocks are distant by at least 2 mm.

The critical current density in the non-copper area of the strand is assumed to be 1500 A/mm^2 at 15 T, 4.2 K for all designs. The variation of the critical current density as a function of field, temperature, stress has been calculated by using the formula given in Annex I.

3.2 Cable configurations

Magnet designs using the same cable in the 2 layers have been studied for the layer design. The copper to non-copper ratio in the strands is 1.25.

In this report, the convention names for the cable dimensions are slightly not usual: the height is equivalent to the generally used word width of the cable; width_inner is the thin edge cable dimension and width_outer is the thick edge dimension.

The various cable configurations investigated are described in the following table:

name	strand diam. [mm]	strand number -	height	width_inner [mm]	width_outer [mm]	Jc (cable + insul.) at 4.2K, 15T [A/mm ²]
CK3	1.25	36	23.4	2.175	2.375	416.3
CK6	1.25	40	26	2.175	2.375	417.1
CK7	1.15	40	23.92	2.001	2.185	411.2
CK8	1.3	40	27.04	2.262	2.47	419.7
CK9	1.3	38	25.688	2.262	2.47	419.4
CK10	1.3	36	24.336	2.262	2.47	419.0

A magnet design using different cable dimensions for inner and outer layer has also been studied in order to have the best use of the quantity of superconducting material (Annex II). The two different cables for inner and outer layers are:

cable name	strand diam. [mm]	strand number	Cu/ non_Cu	height [mm]	width inner [mm]	width outer [mm]	insulation [mm]	Jc_str at 15T, 4.2K [A/mm ²]	Jc_cab at 15T, 4.2K [A/mm ²]
CK1_i	1.35	34	1.25	23.868	2.349	2.565	0.2	666.67	421.2
CK1_o	1.15	40	1.8	23.92	2.001	2.185	0.2	535.71	330.4

3.3 Impact of various parameters: the cable strand number, strand diameter, copper to non copper ratio

Before going to a base line design, several parameters have been varied to see their impact. They are: the cable strand number, strand diameter, copper to non-copper ratio. The variations are sometimes coupled.

The impact study of the various mentioned parameters is made for a two layers dipole design having a bore of 88 mm. For the following impact calculations (paragraph 3.3.1 to 3.3.4.) the iron yoke has been kept at 300 mm thickness.

3.3.1 Impact of strand number and strand diameter

The point here is to check if using cables with bigger strands but less numerous is more efficient. Decreasing the strand diameter gives a thinner cable; this allows then to add more conductors in some blocks of the coils.

The 2 magnet designs compared are CK3 and CK7(block numerology shown in Fig 2)

	Block	1	2	3	4	5	6	7
CK3	conductor nbr.	6	6	4	3	9	10	7
CK7	conductor nbr.	6	7	4	3	10	10	8

This gives:

	strand diam. [mm]	strand number -	Bore field [T]	P_inner [MPa]	P_outer [MPa]	Sum Fx [MN/m]	P_1 [MPa]
CK3	1.25	36	14.19	-155.02	-151.51	15.03	103.84
CK7	1.15	40	14.16	-150.90	-149.10	15.07	106.82

The main field is the bore field in the magnet centre at quench of the conductor reaching the short sample limit (at 4.2 K).

P_inner is the pressure given by summing the azimuthal components of the magnetic forces acting on blocks over the whole inner layer and then dividing it by the cable height.

P_outer is the same but for the outer layer. The effective local pressure on the thin edge of the Rutherford cable can be increased up to 20% compared with the average pressure.

P_1 is the average value of the pressures acting on the width of every conductor of the first block of inner layer (the closest from the mid-plane) supported as a radial pressure by the outer layer supposed to be rigid.

Sum Fx is twice the sum of the x-component of the magnetic forces, over all the conductors of the first quadrant. Sum Fx is then the total horizontal force.

The peak field obtained in both design is the same (14.91 T) and is located in the same place (inside the upper conductor of inner layer, on the inner side).

Comparing the amount of SC material in the two cases, there is a small decrease of 0.3% in CK3 for a field increase of 0.2%.

The effect is marginal.

3.3.2 Impact of strand diameter

Coils with the same number of conductors in the magnet, and same number of strands of different diameters in the cables, are compared.

	strand diam. [mm]	Bore field [T]	P_inner [MPa]	P_outer [MPa]	Sum Fx [MN/m]	P_1 [MPa]
CK6	1.25	14.34	-148.48	-140.21	15.75	110.14
CK8	1.3	14.43	-147.30	-137.39	16.20	108.56

Increasing the strand diameter gives a slightly higher magnetic field. An increase of 8 % in SC material volume leads to an increase of 0.6% in the bore field. Yet the gain in field is low with respect to the effort needed to increase the strand diameter from 1.25 to 1.3, strand diameter in which the aimed current density of 1500 A/mm² would be even more difficult to reach.

3.3.3 Impact of strand number in cable

Coils with the same strand diameter (1.3 mm) and the same number of conductors, but of different cable heights are compared.

	strand number -	Bore field [T] / [%]	P_inner [MPa] / [%]	P_outer [MPa] / [%]	Sum Fx [MN/m] / [%]	P_1 [MPa] / [%]
CK8	40	14.43	-147.30	-137.39	16.20	108.56
CK9	38	-0.68	2.03	3.65	-2.22	-3.22
CK10	36	-1.65	4.25	6.96	-4.89	-6.65

Increasing the number of strand in the cable gives a lower azimuthal pressure on both layers (the cable height is bigger). A reduction of the cable height by 10.9% leads to a field reduction of 1.65%.

3.3.4 Impact of Cu/non Cu ratio

The cable used here is CK6. This gives:

Cu/ non_Cu - / [%]	bore field [T] / [%]	P_inner [MPa] / [%]	P_outer [MPa] / [%]	Sum Fx [MN/m] / [%]	P_1 [MPa] / [%]	copper current density [A/mm ²] / [%]
1.25	14.34	-148.48	-140.21	15.76	110.14	1050.58
-4	0.31	0.69	0.65	0.60	0.65	2.24
-8	0.63	1.36	1.31	1.22	1.30	4.63
-12	0.98	2.09	2.02	1.90	2.01	7.25
-20	1.64	3.52	3.41	3.19	3.38	13.21

Decreasing the copper to non-copper ratio by 20 % gives only 1.64 % gain in main field. We consider that, in our preliminary magnet design studies, it is not a relevant parameter to reach higher magnetic inductions since the copper to non-copper ratio must stay a parameter at disposal for magnet protection studies.

3.3.5 Conclusions

In conclusion on the impact study of a few variables on the conductor, it appears that the main parameter influencing the main field is the overall current density in the coil which is dominated by the critical current density in the non-copper and the insulation thickness.

Both have not been considered as a free parameter because they depend so much on the technology, which will be developed in the frame of the NED program.

With a critical current density of 1500 A/mm² in the non-copper and 0.2 mm thick insulation, the main bore field is limited to 14.4 T in the layer design for a peak field of 15 T on the conductor.

The insulation represents 17% of the total conductor area. The pressure on the broad face of the cable, only due to the electromagnetic forces amounts to 150MPa.

3.4 Base line design for a two layer, 88 mm bore dipole

The base line design of a dipole magnet having a bore of 88 mm is now described below.

It uses the same cable of 40 strands with a diameter of 1.25 mm (cable CK6) in the 2 -layers:

cable name	strand diam. [mm]	strand number	Cu/non_Cu	height [mm]	width inner [mm]	width outer [mm]	insulation [mm]	Jc_str at 15T, 4.2K [A/mm ²]	Jc_cab at 15T, 4.2K [A/mm ²]
CK6	1.25	40	1.25	26	2.175	2.375	0.2	666.67	417.1

The number of conductors is 19 for the inner layer and 26 for the outer layer.

The iron yoke thickness is 350 mm.

The outer cylinder is 28 mm thick.

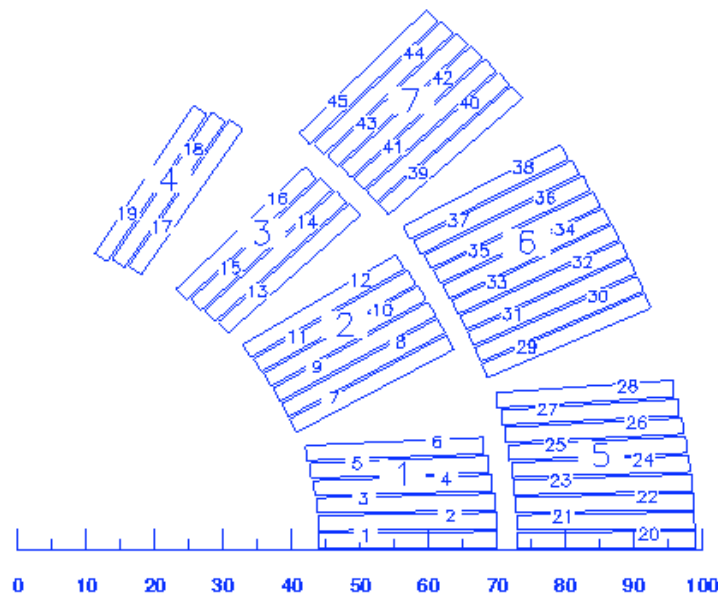


Fig. 2 Magnet cross section (design CK6)

3.4.1 Magnetic aspects

3.4.1.1 Magnetic field distribution

The magnet configuration is the design CK6 with a first optimization to decrease the multipole levels which are not yet satisfactory and must still be reduced. This gives the following magnetic field distribution.

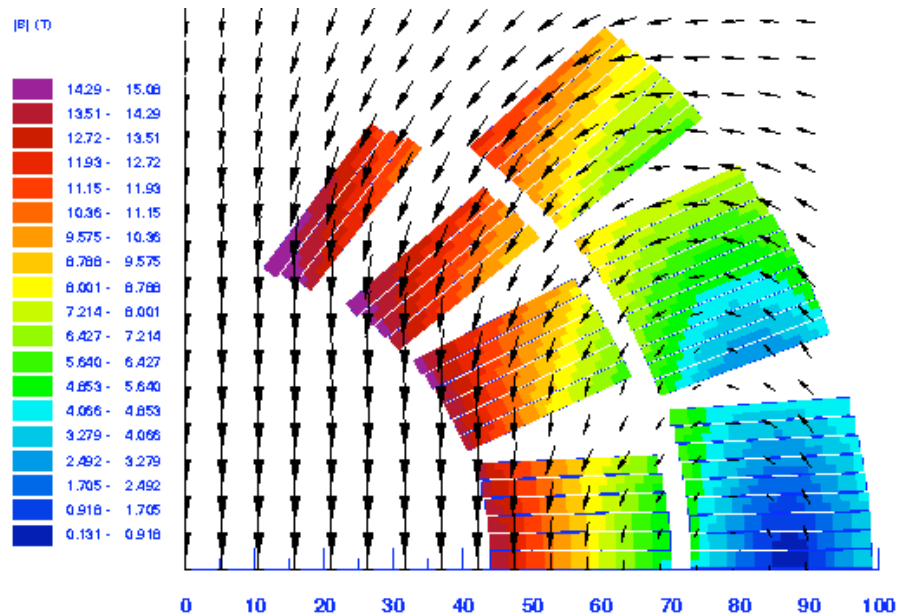


Fig. 3 Magnetic induction distribution (design CK6_opt)

Central field at 4.2 K [T]	I [A]	b1 -	b3 -	b5 -	b7 -	L [mH/m]	E/m [kJ/m]	copper current density [A/mm ²]
-14.42	28530	10000	3.986	-0.035	0.012	4.43	1803.67	1046.2

The reference radius for the multipole calculation is 10 mm. Further optimization is required to further decrease the multipole levels, for an accelerator type magnet. This optimization is not in the scope of this report due to the uncertainty on the final cable dimensions which will be known at the end of the development programme on the conductor.

3.4.1.2 Peak fields in blocks and load lines

It has to be pointed out that the current density in the non-copper is 1500 A/mm² at 15 T, 4.2 K; 3000 A/mm² at 12 T, 4.2 K and that a cable degradation of 10% is assumed.

Block number	Peak field [T]	% on load line at 4.2 K [%]	Peak/Central [%]
1	14.22	95.1	98.6
2	14.35	95.8	99.5
3	14.72	98.0	102.1
4	15.09	100.0	104.6
5	6.17	49.6	42.8
6	8.97	65.4	62.2
7	12.02	82.7	83.3

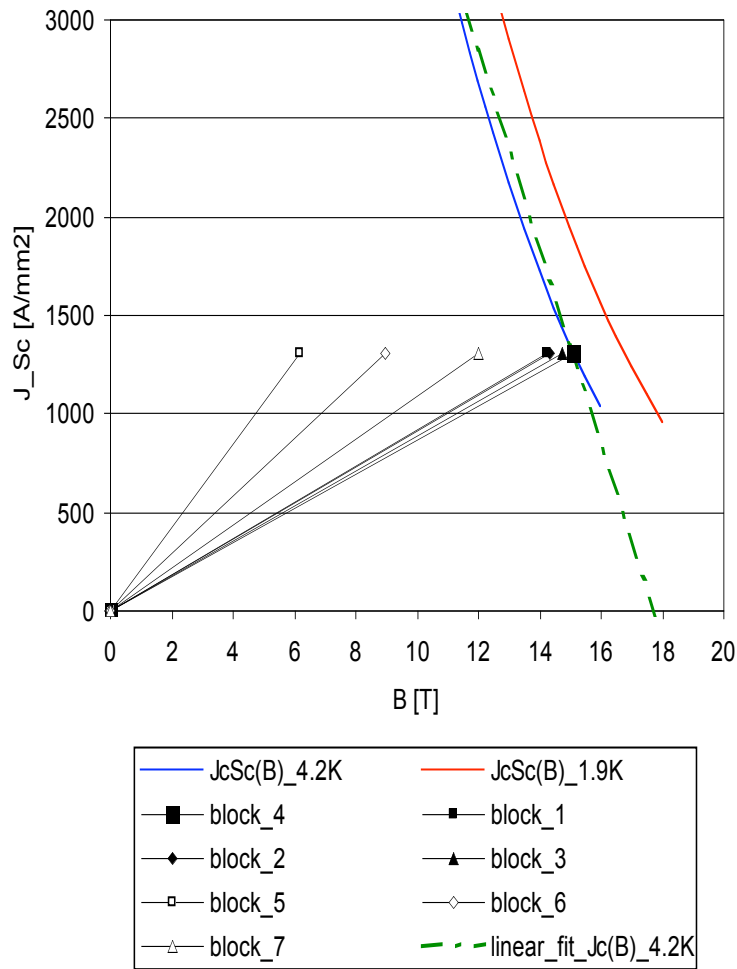


Fig. 4 Load lines (design CK6_opt)

With the magnet working in the superfluid helium, one could reach a maximum bore field of 15.3 T, with 16.1 T of peak field at short sample limit.

3.4.1.3 Magnet transfer function

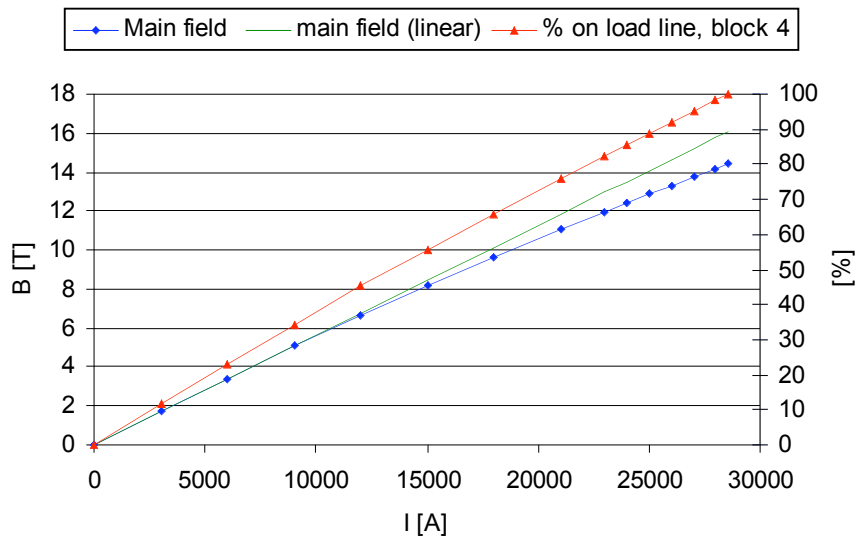


Fig. 5. Transfer function (design CK6_opt)

The difference, due to the iron saturation effect, between the actual central field obtained in the magnet and the linear extrapolation of the low field load line is of 11.39 % at the quench field of 14.42 T in the bore.

3.4.1.4 *Magnetic field leakage*

The iron yoke is made of Armco iron ($M_s = 2.11$ T), the leakage magnetic field calculated on the mid-plane just outside the shrinking cylinder is :

iron yoke thickness [mm]	central field [T]	I [A]	B leakage [T]
350	14.42	28530	0.072

3.4.2 *Electromagnetic Forces*

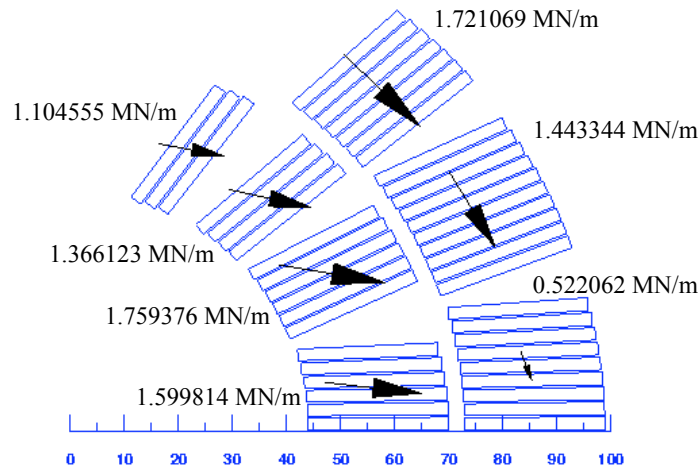


Fig. 6 *Magnetic forces (design CK6_opt) -(Only the 3rd digit is significant).*

P_inner [MPa]	P_outer [MPa]	P_1 [MPa]	Sum Fx [Tonnes/m]
-147.830	-141.226	111.068	1585.6

For the P_inner and P_outer definitions, see paragraph 3.3.1.

3.4.3 Losses in conductors

3.4.3.1 Hysteretic losses

For the cable used in design CK6_opt, we have:

d_f [μm]	h [mm]	$\langle w \rangle$ [mm]	Cu/non_Cu -
50	26	2.275	1.25

Taking the parameterisation described in Annex I for the superconductor critical density and assuming a cycle from 0.01 to 14 T and back to 0.01 T, we get for a one meter long magnet:

$$Q_{\text{hyst}} = 15444 \text{ J/m/cycle}$$

3.4.3.2 Inter-filament losses

Cu/non_Cu -	$L_{p,f}$ [mm]	ρ_{eff} [$\Omega\cdot\text{m}$]	RRR -
1.25	30	6.80E-11	250

Here $\rho_{\text{eff}} = \rho_{\text{matrix}}$: we assume that half of the filaments contribute to the transverse resistivity of the matrix. The ramp rate for the field increase is 0.1 T/s. The inter-filament losses are difficult to calculate in a Nb₃Sn strand because of the presence of bronze and copper. The results given for a one meter long magnet are thus only indicative and valid for comparison purposes.

We then get: $P_{\text{if}} = 12.471 \text{ W/m}$

$\tau_{\text{if}} = 211 \text{ ms}$ (time constant of the inter-filaments coupling currents)

The high value of τ is governed by the assumed high values of $L_{p,f}$ and RRR of 30mm and 250 .

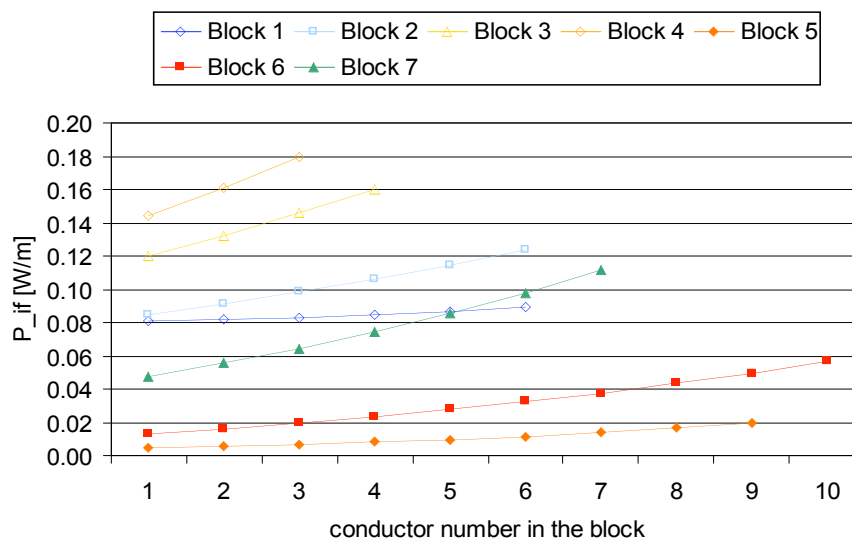


Fig. 7 Inter-filaments coupling power loss in each conductor (design CK6_opt)

The upper conductor of each layer has the higher inter-filament losses.

3.4.3.3 Inter-strands coupling losses

For a magnetic field ramp rate of 0.1 T/s, we get:

Lp,s [mm]	h [mm]	<w> [mm]	strand number -	Ra [μohm]	Rc [μohm]	P_a [W/m]	P_c [W/m]
182	26	2.275	40	1000	100	0.005	3.964
				1	100	5.000	3.964

(The losses in block 5 have been neglected). The indicated losses are per meter of magnet length. The adjacent resistance between strands have been varied between two extremes values. The lowest value of 1 μΩ could correspond to sintered strands after full reaction.

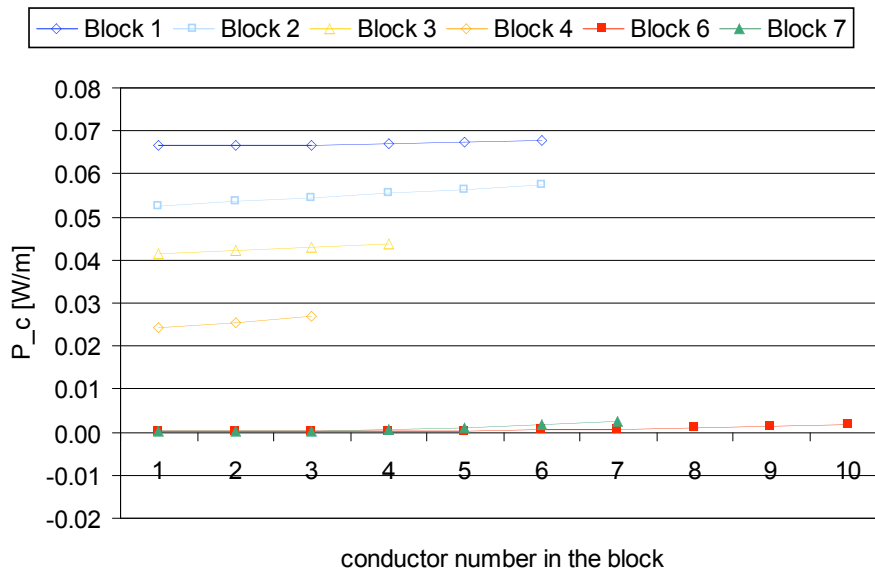


Fig. 8 Inter-strands coupling losses Pc per meter of magnet length (through crossing resistance only) for Rc = 100 μΩ (design CK6_opt)

The higher inter-strand losses are located in the first 2 blocks of the inner layer.

3.4.4 Overall Characteristics of the 88 mm, two layers, base line design

Layer design: keystone cable
 Cable: 40x1.25 mmφ

Field [T] / Current [A]	L [mH/m]	E/m [kJ/m]	Max pressure [MPa]	Fx, result. [MN/m]	Pc - 100μΩ- 0.1T/s [W/m]	Pa - 1μΩ- 0.1T/s [W/m]	Overall diameter [mm]
14.42 / 28660	4.4	1810	148	15.8	3.964	5	1004

3.4.5 *Considerations on the mechanical design*

As already mentioned, the approach for the mechanical design is similar to the one used for the MFRESCA magnet [4].

One of the major items is to keep the horizontal gap closed when the magnet is powered. The iron is designed with a horizontal gap of $\sim 230 \mu\text{m}$ [9].

After welding the shrinking cylinder with an azimuthal stress of $\sim 160 \text{ MPa}$, the iron gap is closed at its external radius over 70 mm. The mating pressure does not exceed the iron Yield Strength. At cold temperature, the yoke is fully closed and stays closed under the action of the magnetic forces.

This entire scheme depends strongly on the values of the elastic modulus of the coils at room temperature and at cold conditions, and depends also on the integrated thermal expansion of the coils.

The values taken for the estimations are:

- coil elastic modulus at room temperature of 33 GPa
- coil elastic modulus at cold conditions of 45 GPa
- coil integrated thermal contraction of 0.0039 [10].

The magnet is then built with an interference of $65 \mu\text{m}$ between yoke and collars at room temperature. The anti-ovalization of the collars is of $150 \mu\text{m}$.

The average coil stresses vary from 22 MPa at room temperature, 80 MPa after yoking, to 50 MPa at cold conditions.

At 15 T, the coil has lost stresses at the upper conductor of the layer but the 150 MPa of the magnetic forces are added to the mid-plane conductor, which sees then an average compression of 200 MPa. The maximum local stress on the inner radius of the layer can be 20 % higher.

In conclusion of the pre-mechanical analysis based on the MFRESCA design, it appears that the layer design could lead to a high compression stress of $\sim 240 \text{ MPa}$.

The magnetic stresses are added to the pre-stress in the coils in the layer design. The question remains: how much pre-stress do we need? Do we accept the loss of contact at the upper conductor of the layer by reducing the pre-stress in the coils?

3.5 **A 88 mm dipole with 2 types of cables**

The annex II describes a 88mm dipole having 2 types of cable, one for the inner layer and another one for the outer layer.

The cable for the inner layer consists of 34 strands of 1.35mm diameter and a copper to non-copper of 1.25.

The cable for the outer layer consists of 40 strands of 1.15 mm diameter and a copper to non-copper of 1.8.

This design having more copper in the outer layer could be interesting for the quench protection. It makes also a better use of the superconducting material.

This case has not been considered for the NED program since it would have involved the development of 2 types of cables.

The quenching bore field of 14.45 T and the electro-magnetic characteristics are similar to the design with the same cable in the 2 layers.

The pressures on the conductors are increased up to 14% due to the reduction in height of the conductors.

3.6 Base line design for a two layer, 130 mm bore dipole

The cable used here is cable CK6:

cable name	strand diam. [mm]	strand number	Cu/non_Cu	height [mm]	width inner [mm]	width outer [mm]	insulation [mm]	Jc_str at 15T, 4.2K [A/mm ²]	Jc_cab at 15T, 4.2K [A/mm ²]
CK6	1.25	40	1.25	26	2.175	2.375	0.2	666.67	417.1

The coil configuration is kind of homothetic to the 88 mm aperture design CK6.

The iron yoke is 500 mm thick, and its internal radius is 145 mm.

The outer cylinder is 37 mm thick.

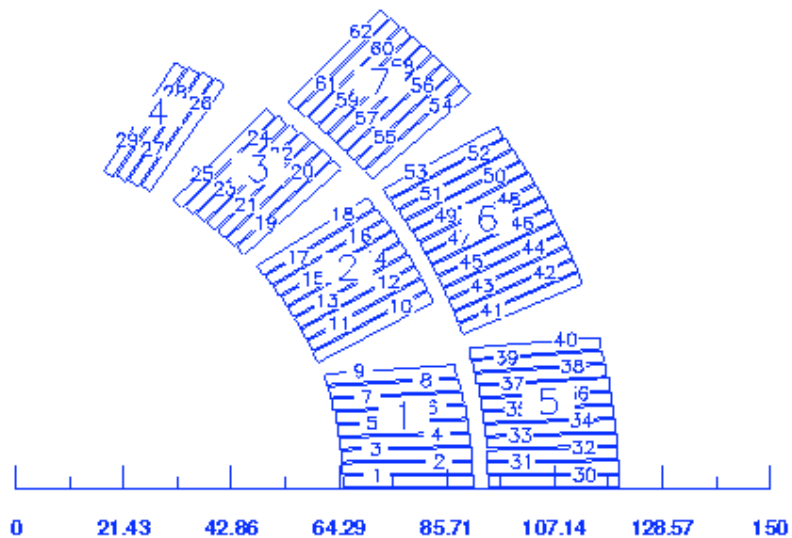


Fig. 9 Layer design, 130 mm – aperture, cross section (design CK11)

3.6.1 *Magnetic aspects of a 130 mm layer design dipole*

Central field at 4.2K [T]	I [A]	b1 -	b3 -	b5 -	b7 -	L [mH/m]	E/m [kJ/m]	copper current density [A/mm ²]
14.31	26310	10000	-4.981	-0.033	0.003	8.71	3013.38	964.8

The reference radius for the multipole calculation is 10 mm.
 The coil configuration has not been optimized to decrease the multipole levels.

Block number	Peak field [T]	% on load line [%]	Peak/Central [%]
1	13.98	92.6	97.7
2	14.25	94.1	99.6
3	14.87	97.6	103.9
4	15.29	100.0	106.8
5	5.83	46.6	40.7
6	8.81	63.4	61.6
7	12.40	83.7	86.6

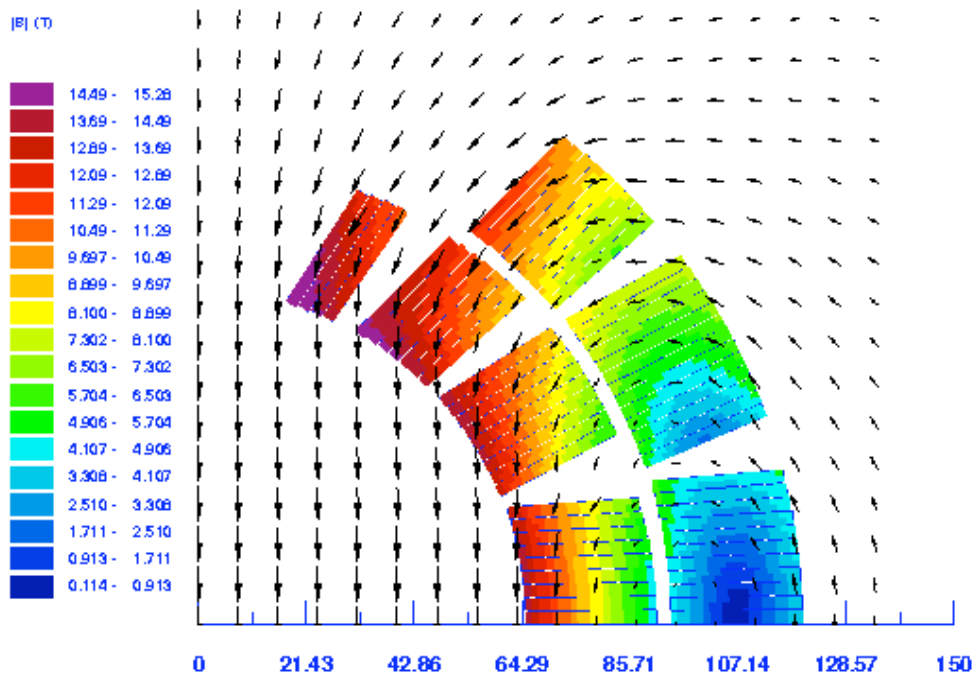


Fig. 10 Magnetic induction distribution (design CK11)

The residual magnetic field on the mid-plane just outside the shrinking cylinder is 0.03 T.

3.6.2 Electro-magnetic force aspects of a 130 mm layer design dipole

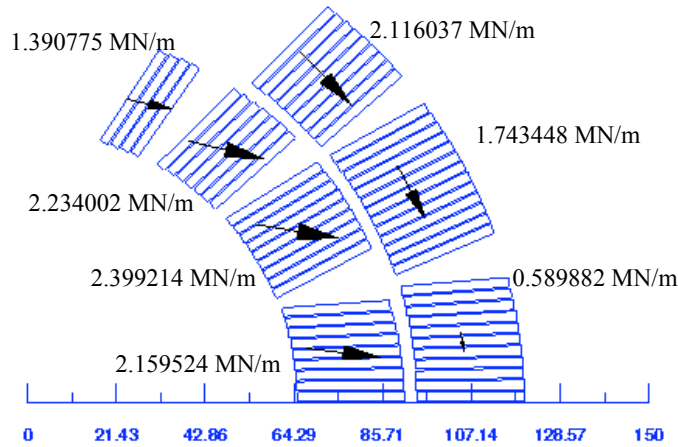


Fig. 11 Magnetic forces distribution (design CK11) -(Only the 3rd digit is significant).

P_inner [MPa]	P_outer [MPa]	P_1 [MPa]	Sum Fx [MN/m]
-214.871	-170.815	99.642	20.9

3.6.3 Conductor losses in a 130 mm layer design dipole

3.6.3.1 Hysteretic losses

For the cable used in design CK11, we have:

d _f [μm]	h [mm]	<w> [mm]	Cu/non_Cu -
50	26	2.275	1.25

Taking the parameterisation described in Annex 1 for the superconductor critical density and assuming a cycle from 0.01 to 14 T and back to 0.01 T, we get for the whole magnet:

$$Q_{\text{hyst}} = 21278 \text{ J/m/cycle}$$

For 50 cycles from 11 T to 11.5 T and back to 11T, we get for the whole magnet:

$$Q_{\text{hyst}} = 10084 \text{ J/m}$$

3.6.3.2 Inter-filament losses

Cu/non_Cu -	L _{p,f} [mm]	ρ _{eff} [Ω.m]	RRR -
1.25	30	6.80E-11	250

Here $\rho_{\text{eff}} = \rho_{\text{matrix}}$: we assume that half of the filaments contribute to the transverse resistivity of the matrix. (see 3.4.3.2)

For a field ramp rate of 0.1 and 0.5 T/s we get respectively in one-meter long magnet:

$$P_{\text{if}} = 18.67 \text{ W/m and } 466.71 \text{ W/m}$$

$$\tau_{\text{if}} = 211 \text{ ms (time constant of the inter-filaments coupling currents)}$$

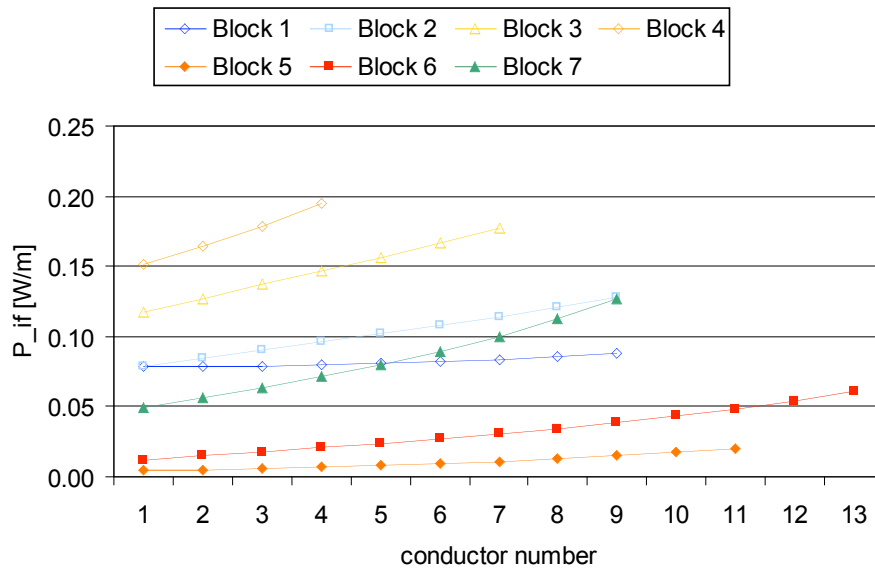


Fig. 12 Inter-filaments losses in each conductor (ramp rate of 0.1 T/s)(design CK11)

3.6.3.3 Inter-strands coupling losses

For a field ramp rate of 0.1 T/s we have per meter of magnet length:

Lp,s [mm]	h [mm]	<w> [mm]	strand number	Ra [μohm]	Rc [μohm]	P_a [W/m]	P_c [W/m]
182	26	2.275	40	1000	100	0.006	9.011
				1	100	6.818	9.011

And for a field ramp rate of 0.5 T/s we have per meter of magnet length:

Lp,s [mm]	h [mm]	<w> [mm]	strand number	Ra [μohm]	Rc [μohm]	P_a [W/m]	P_c [W/m]
182	26	2.275	40	1000	100	0.170	225.270
				1	100	170.467	225.270

(The losses in block 5 have been neglected).

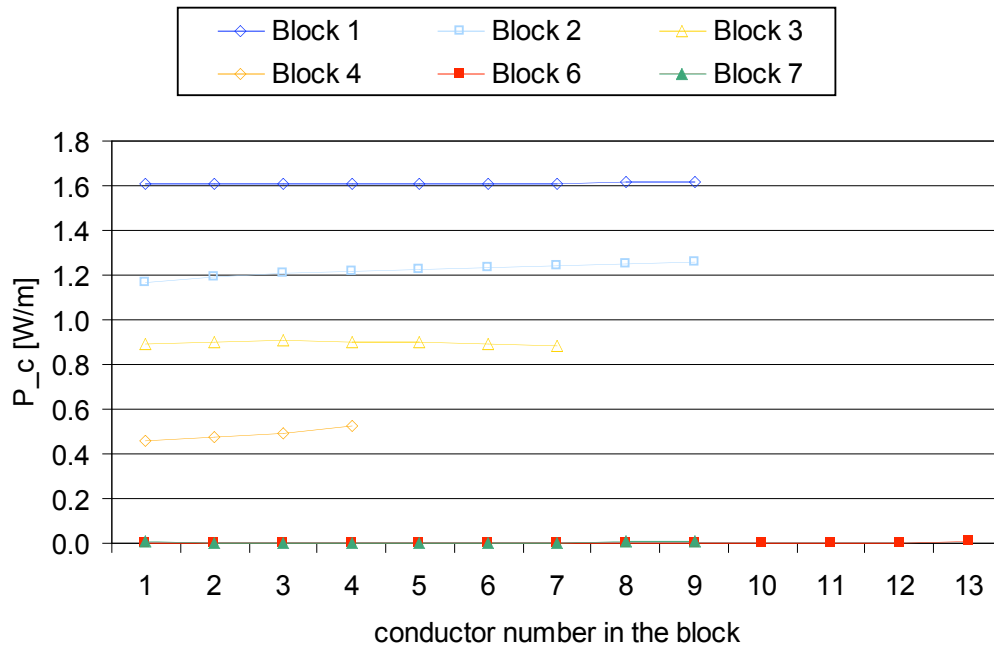


Fig. 13 Inter-strands coupling losses (through crossing resistance only, for a 0.5 T/s field ramp rate and $R_c = 100\mu\Omega$) (design CK11)

3.6.4 Overall Characteristics of the 130 mm, two layers, base line design

Layer design: keystone cable

Cable: 40x1.25 mm ϕ

Field [T] / Current [A]	L [mH/m]	E/m [kJ/m]	Max pressure [MPa]	F _x , result. [MN/m]	P _c - 100 $\mu\Omega$ - 0.1T/s [W/m]	P _a - 1 $\mu\Omega$ - 0.1T/s [W/m]	Overall diameter [mm]
14.3 / 263100	8.7	3013	215	20.9	9	6.8	1364

3.7 Base line design for a two layers, 160 mm bore dipole

The cable used here is cable CK6:

cable name	strand diam. [mm]	strand number	Cu/ non_Cu	height [mm]	width inner [mm]	width outer [mm]	insulation [mm]	J _c _str at 15T, 4.2K [A/mm ²]	J _c _cab at 15T, 4.2K [A/mm ²]
CK6	1.25	40	1.25	26	2.175	2.375	0.2	666.67	417.1

The coil configuration is kind of homothetic to the 88 and 130 mm aperture designs.

The iron yoke is 640 mm thick, and its internal radius is 160 mm.

The outer cylinder is 44 mm thick.

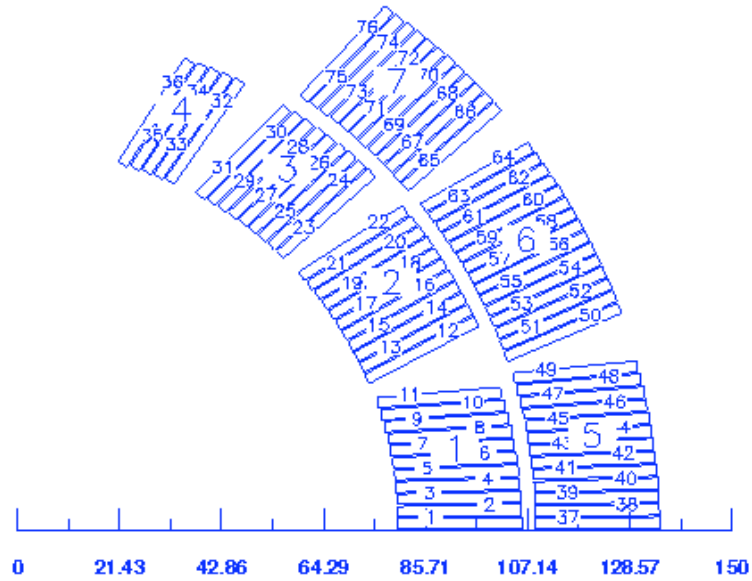


Fig. 14 Layer design, 160 mm – aperture, cross section (design CK16)

3.7.1 Magnetic aspects of a 160 mm layer design dipole

Central field [T]	I [A]	b1 -	b3 -	b5 -	b7 -	L [mH/m]	E/m [kJ/m]	copper current density [A/mm ²]
14.19	24810	10000	-5.071	-0.012	-0.001	13.18	4056.79	909.8

The reference radius for the multipole calculation is 10 mm.

The coil configuration has not been optimized to decrease the multipoles levels.

Block number	Peak field [T]	% on load line [%]	Peak/Central [%]
1	13.76	90.6	96.9
2	14.10	92.5	99.3
3	14.87	96.8	104.8
4	15.43	100.0	108.7
5	5.78	45.5	40.8
6	8.62	61.5	60.7
7	12.83	85.3	90.4

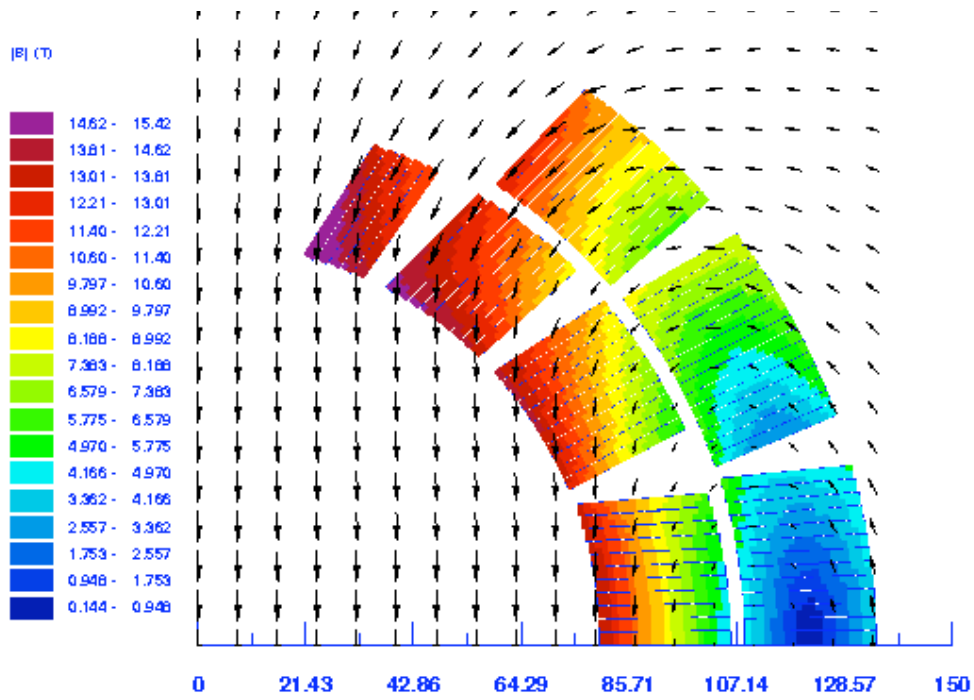


Fig. 15 Magnetic induction distribution (design CK16)

The residual magnetic field on the mid-plane at the shrinking cylinder edge is 0.015 T.

3.7.2 *Electro-magnetic force aspects of a 160 mm layer design dipole*

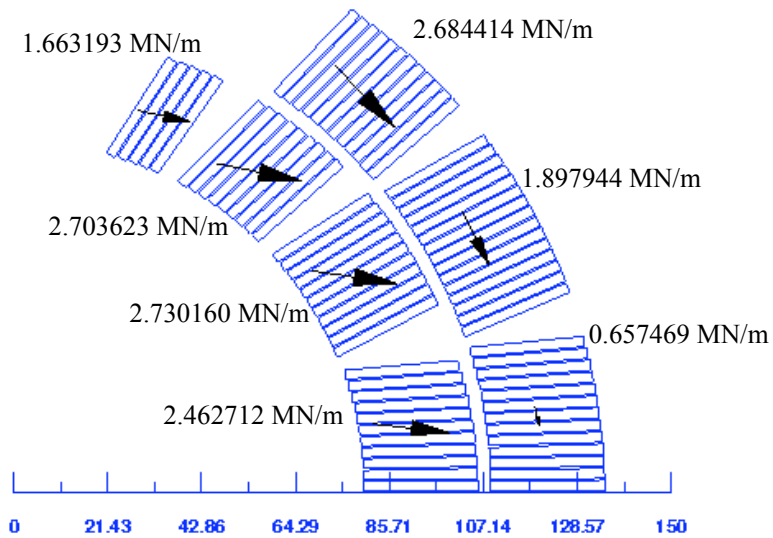


Fig. 16 Magnetic forces distribution (design CK16) -(Only the 3rd digit is significant).

P_inner [MPa]	P_outer [MPa]	P_1 [MPa]	Sum Fx [MN/m]
-252.126	-201.065	92.875	24.56

3.7.3 Conductor losses in a 160 mm layer design dipole

3.7.3.1 Hysteretic losses

For the cable used in design CK16, we have:

d_f [μm]	h [mm]	$\langle w \rangle$ [mm]	Cu/non_Cu -
50	26	2.275	1.25

Taking the parameterisation described in Annex 1 for the superconductor critical density and assuming a cycle from 0.01 to 14 T and back to 0.01 T, we get for the whole magnet:

$$Q_{\text{hyst}} = 26083 \text{ J/m/cycle}$$

For 50 cycles from 11 T to 11.5 T and back to 11T, we get for the whole magnet:

$$Q_{\text{hyst}} = 12361 \text{ J/m}$$

3.7.3.2 Inter-filament losses

Cu/non_Cu -	$L_{p,f}$ [mm]	ρ_{eff} [$\Omega \cdot \text{m}$]	RRR -
1.25	30	6.80E-11	250

Here $\rho_{\text{eff}} = \rho_{\text{matrix}}$: we assume that half of the filaments contribute to the transverse resistivity of the matrix.

For a ramp rate for the field increase of 0.1 and 0.5 T/s we get respectively:

$$P_{\text{if}} = 23.59 \text{ W/m and } 589.71 \text{ W/m}$$

$$\tau_{\text{if}} = 211 \text{ ms (time constant of the inter-filaments coupling currents)}$$

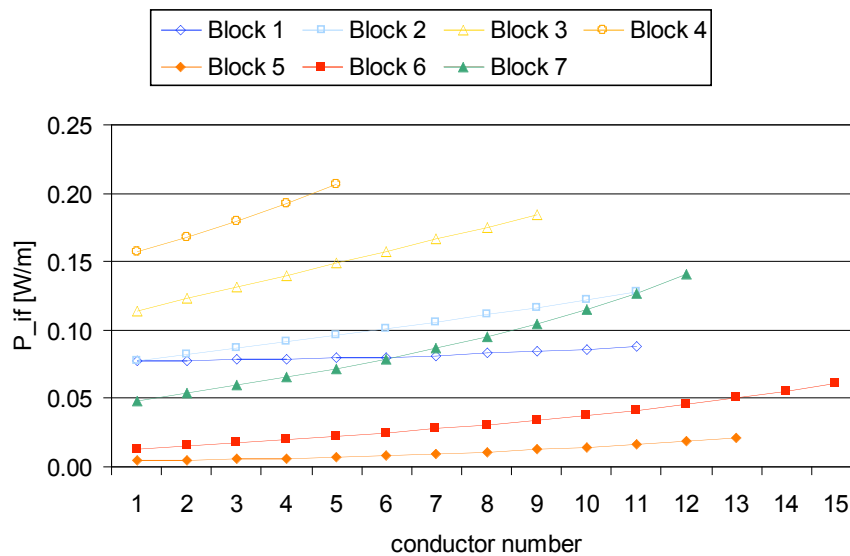


Fig. 17 Inter-filaments losses in each conductor (ramp rate of 0.1 T/s)(design CK16)

3.7.3.3 Inter-strands coupling losses

For a ramp rate for the magnetic field increase of 0.1 T/s we have:

L _{p,s} [mm]	h [mm]	<w> [mm]	strand number -	R _a [μohm]	R _c [μohm]	P _a [W/m]	P _c [W/m]
182	26	2.275	40	1000	100	0.008	11.585
				1	100	8.397	11.585

And for a ramp rate for the magnetic field increase of 0.5 T/s we have:

L _{p,s} [mm]	h [mm]	<w> [mm]	strand number -	R _a [μohm]	R _c [μohm]	P _a [W/m]	P _c [W/m]
182	26	2.275	40	1000	100	0.209	289.625
				1	100	209.914	289.625

(The losses in block 5 have been neglected).

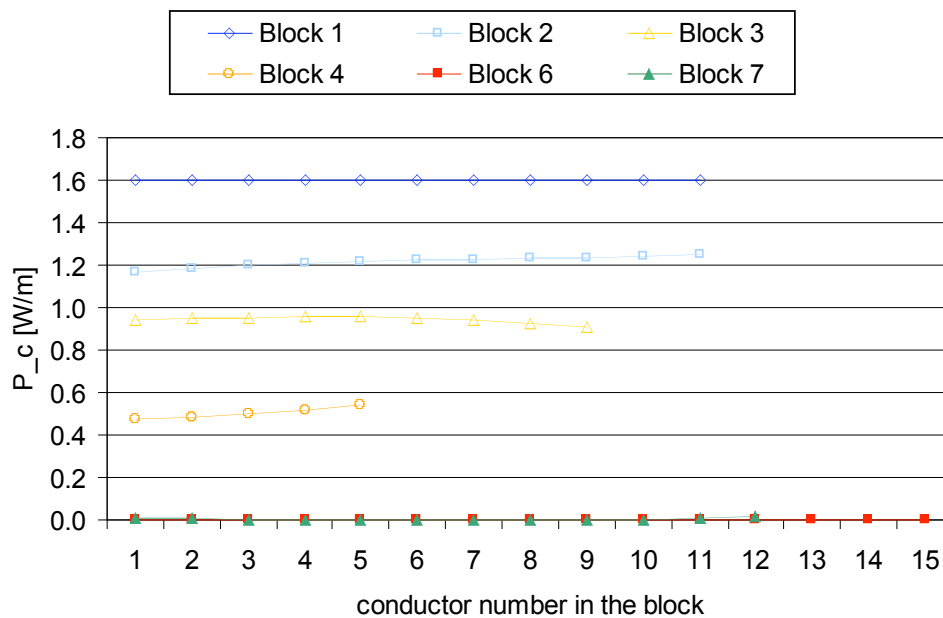


Fig. 18 Inter-strands coupling losses (through crossing resistance only, for a 0.5 T/s field ramp rate and R_c = 100 μΩ) (design CK16)

3.7.4 Overall Characteristics of the 160 mm, two layers, base line design

Layer design: keystone cable

Cable: 40x1.25 mmφ

Field [T] / Current [A]	L [mH/m]	E/m [kJ/m]	Max pressure [MPa]	F _x , result. [MN/m]	P _c - 100μΩ- 0.1T/s [W/m]	P _a - 1μΩ- 0.1T/s [W/m]	Overall diameter [mm]
14.2 / 24810	13.2	4056	252	24.5	11.6	8.4	1688

4. SLOT DESIGN

4.1 Magnet general layout

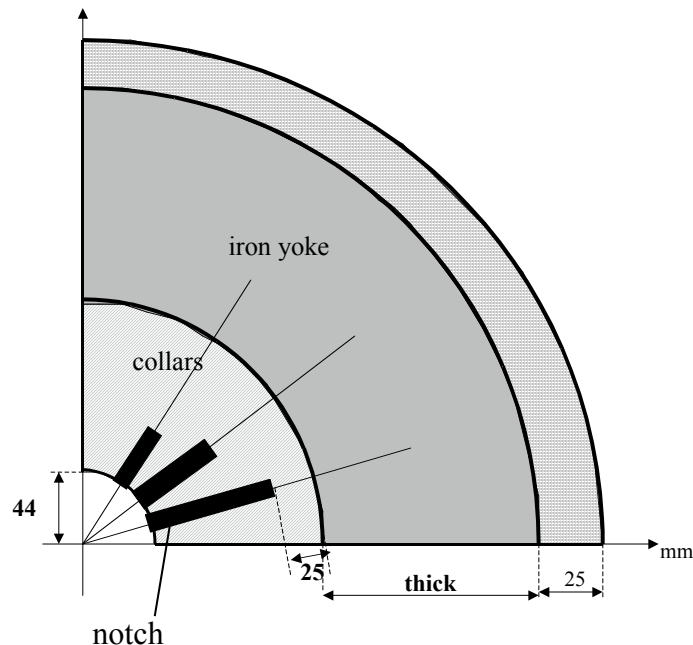


Fig. 19 Magnet cross section (slot design)

In this design, the rectangular conductors are located in radial notches machined in a metallic structure.

The winding is performed by inserting the cables in the metallic structure, positioned horizontally, with the notches in position open upwards.

The ends are rather difficult to wind since the cable sees there a hard bending. Passing from one notch to the other will occur in the ends where the conductor from the top of a notch goes to the bottom of the other notch.

This kind of winding in an open structure and not on a mandrel has already been made at BNL (Isabelle) for a single layer design. A magnet using the slot design type has already been built at CEA Saclay [11], [12] with a NbTi cable.

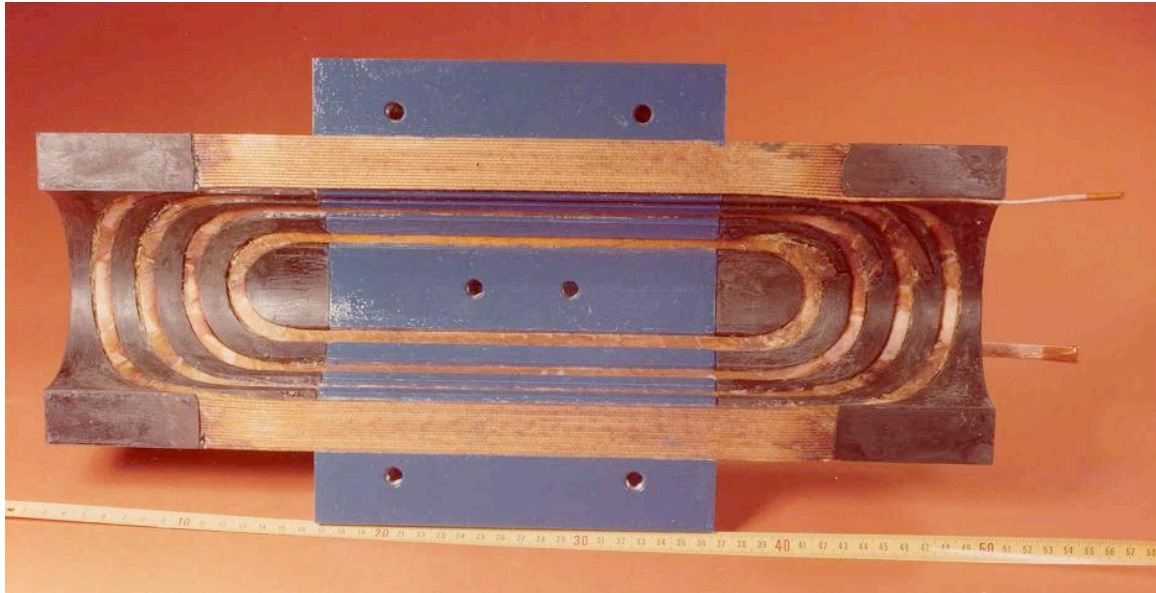
It needs a good and clever tooling. This type of approach could be made with the Nb₃Sn cables, which seem to be less “nervous” than the NbTi cables.

After winding, the reaction and the impregnation could be performed in the same metallic structure, which becomes a mechanical support for the electro-magnetic forces. Due to the volume expansion of the Nb₃Sn at reaction, the conductor, located in the closed volume of the notch could need less pre-stress at assembly. Bladders could be incorporated in the notches to introduce a pre-stress if needed. The external mechanical structure would be the same as for the layer design. The two poles are associated by a lateral welding. The yoke is split horizontally and contained in a shrinking cylinder.

Cooling of the conductors in the notches could be made with copper drains.

A difficulty could be the quench protection for long magnets, which would require quench heaters incorporated in the notches. In this design, the inter-strand losses are reduced since the field is \sim parallel to the broad face of the cables. The quench back effect is then reduced except if the adjacent resistance between the strands of the cables is small.

Picture 1 shows a model magnet investigated at CEA Saclay [11]:



Picture 1 Model magnet built at CEA Saclay

The advantages of the slot design compared to layer design are: more free space on the mid-plane, and about twice more margin in field on the block closest to the mid-plane with respect to the upper block as in layer magnets, which could be interesting for beam losses. The field margins are calculated at the short sample limit on the field load line.

For the slot designs considered here, the magnet aperture is 44 mm. There is 3 mm space between two adjacent blocks (wound with the same cable). The magnet is made of three blocks placed in radial notches for a 88mm dipole.

A minimum thickness of 25mm is maintained between coil and yoke

As an approach for the design, the different lengths of blocks (or notches) are correlated to get approximately an ellipsoidal shape.

4.2 Conventions and naming for the electro-magnetic force calculations

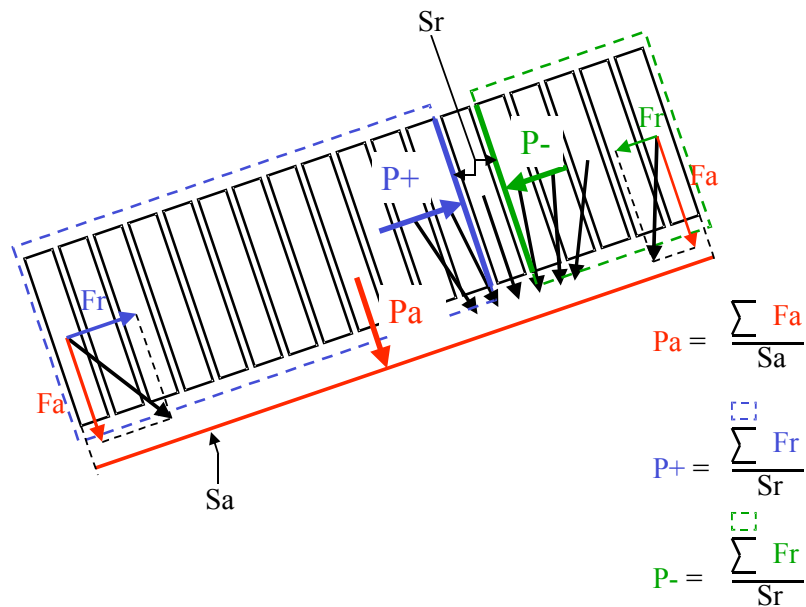


Fig. 20 Notch cross section, definition of calculated pressures.

P_+ is the pressure given by the sum of all radial components of magnetic forces acting on the conductors of the notch and oriented towards the outside. P_- is the same but for blocks with forces oriented towards the inside of the structure. The introduction of P_+ and P_- as defined in Fig 20 allows to calculate the localization of maximum pressure between two conductors in the block structure.

In all the designs investigated $P_+ > P_-$, this means that conductors are pushed towards the bottom of the notch. F_{notch} is the resulting magnetic force on the bottom of the notch. This force is always oriented towards the outside of the structure.

P_a is the pressure given by the sum of all azimuthal components of magnetic forces acting on all the conductors of the notch (they are all oriented towards the mid-plane of the magnet).

All calculations are made both with software Roxie [6] and by analytical means [7].

4.3 Variations of design parameters for slot magnets

Annex III, IV and V present the results of parametric studies for slot designs of 88 mm and 160 mm aperture.

The critical current density of the Nb_3Sn used is again assumed to be 1500 A/mm^2 at 15 T, 3000 A/mm^2 at 12 T, at 4.2 K.

The strand diameter is 1.25 mm and the copper to non-copper ratio is 1.25.

The insulation thickness is 0.2 mm.

Several parameters, such as notch angle, notch length, number of notches, cable height, are varied in order to draw some general conclusions about the slot design type. The main difficulty is that most of these parameters are not independent, yet it is possible to catch a glimpse of the potentiality of the slot design.

4.3.1 Impact of the number of conductors

The number of conductors in each notch of the design is increased, while the angles of the notches, the cable used (CR2) and the magnet aperture (88mm) are kept identical (Annex III). For the various design investigated in this section, the number of conductors in each notch are correlated in such a way that the overall shape of the coils can be approached with ellipses. For all the designs, the ellipses are homothetic: they have the same eccentricity: $e = 0.777$).

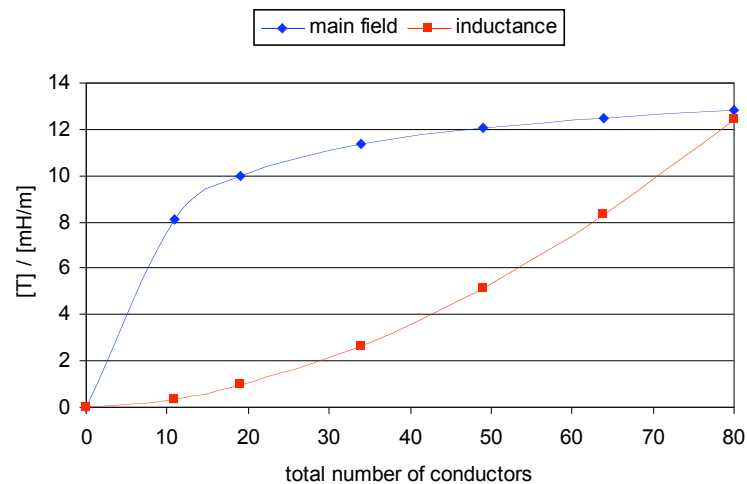


Fig. 21 homothetic growth of a slot design (3 notches with cable CR2)

The saturation in the main field curve, in the previous graph, shows that the conductors at the bottom of the notches are less effective than the ones closer to the aperture.

4.3.2 Impact of notch angle and notch length

The angle of a single notch in the design, or its length, is now changed, while the other notches are kept identical (Annex IV).

The study is made for a slot design of 88 mm aperture with 3 notches of cable CR2, and the iron yoke is modelled as infinite and of infinite permeability.

4.3.2.1 *Variation of the angle of one notch (Annex IV, IV.2.1.)*

The numbers of conductors in blocks are respectively 33, 25,15 for notches 1, 2, 3.

A variation of 10 degrees in the angle of any of the three notches gives a relatively low variation of the main field:

- a variation of 10 degrees of notch 1 angle gives a bore field reduction of 2.8% and an increase by 16% of the maximum pressure on the conductor in notch 1.
- a variation of 10 degrees of notch 2 angle gives a bore field reduction of 5.2% and an increase by 20% of the maximum pressure on the conductor in notch 2.
- a variation of 10 degrees of notch 2 angle gives a bore field increase of 0.1% and an increase by 20% of the maximum pressure on the conductor in notch 3.

As shown in the tables of Annex IV, the multipole harmonics are very sensitive to these angle changes. In particular the B3 and B7 coefficients are very sensitive to variation of notch 2 angle: a variation of 10 degrees (+33.3%) of the notch 2 angle gives a 660% increase of the B3 coefficient and a 3272% increase of the B7 coefficient.

The B5 coefficient is more sensitive on a variation of the notch 1 angle: 458% increase for 10 degrees variation in notch 1 angle, compared to 25% for the same variation on notch 2 angle.

4.3.2.2 *Variation of the length of one notch (Annex IV, IV.2.2.)*

The length of a notch, that is to say the number of conductors in the notch, is changed, while the two other notches are kept identical.

Notches angles are kept constant and are respectively 10, 30 and 50 degrees for notches 1, 2 and 3.

The tables show a low sensitivity of the main field to the notch length (this refers to the saturation shown in Fig. 21):

- Passing from 28 to 43 conductors in notch 1, the bore field increases by 2% with a number of conductors in notches 2 and 3 of 25 and 15.

The inner radius of the iron yoke is determined by the length of the longer notch, which here is always notch 1. The inner radius of the iron yoke passes from 140 to 179 mm.

- Passing from 22 to 31 conductors in notch 2, the bore field increases by 2.2% with a number of conductors in notches 1 and 3 of 35 and 15.

The inner radius of the iron yoke is 153 mm.

- Passing from 12 to 21 conductors in notch 3, the bore field decreases by 6.5% with a number of conductors in notches 1 and 2 of 35 and 15.

The inner radius of the iron yoke is 153 mm.

The multipoles coefficients are less sensitive to the notch length than to the notch angle: the variations are all below 65% for B3, B5 and B7.

The B3 coefficient is sensitive mostly to variation in the length of notch 1 and 3, and especially notch 3. Coefficients B5 and B7 show sensitivities below 10% for a variation, of at maximum 50%, of the length of any of the 3 notches.

4.3.3 Impact of notch width

The varying parameter is now the notch width, that is to say the height of the cable.

The impact study of the notch width (or cable height) on a 88 mm aperture magnet (Annex IV, IV.2.3.) is not significant enough since the variation range of the cable height is limited to 20% because of the little space available between notches in the 88 mm design.

The same study is carried out on a magnet with 160 mm aperture (and a finite iron yoke of 640 mm thick) (Annex V, V.2.).

The magnets have all 3 notches of angles 12, 34 and 56 degrees.

The total amount of superconductor in the design is kept constant.

Doubling the cable height gives a 10% increase of the main field while the self-inductance is divided by a factor 3.5 (and the quench current is approximately doubled).

Increasing the cable height gives less long notches, the main field benefits from the fact that the iron yoke is closer and that the conductors are more efficiently used (closer to the aperture).

Increasing the cable height allows also to decrease the number of conductors and so the self-inductance, which can be an issue for protection aspects.

Concerning the magnetic forces aspects, P+ decreases (-37% from 196.7 to 122.4 MPa) due to a lower cable width; on the contrary P-azi increases from -17.1 to -44.2 MPa due to larger cable height.

4.3.4 Impact of notch number

The varying parameter is the number of notches of the magnet, while the total number of conductors remains unchanged (Annex V, V.1.).

The cable used here is CR2 (with 10% critical current degradation due to cabling).

The aperture of the magnet is 160 mm and the iron yoke thickness is 640mm

Passing from a design with 3 notches to 5 notches (with the same cable CR2) gives a 3.3% increase of the main field, the self-inductance remaining the same.

Increasing the number of notches gives less long notches, the main field benefits a little from the fact that the iron yoke is closer and that the conductors are more efficiently used (closer to the aperture).

Concerning the magnetic forces aspects, passing from 3 to 5 notches gives a decrease of about 48% of the maximum pressure (on a conductor) in the structure (from 205.5 to 111.7 MPa). The maximum force transmitted to the bottom of a notch in the design is also decreased by a factor 2.

Increasing the number of notches allows to better distribute the magnetic forces in the structure and so helps decreasing Pmax and F_notch max.

4.4 Base line design of a slot type dipole of 88 mm aperture

The cable used is CR4.

We assume a degradation of the cable critical current due to cabling of 10%.

cable name	strand diam. [mm]	strand number	Cu/non_Cu	height [mm]	width [mm]	insulation [mm]	Jc_str at 15T, 4.2K [A/mm ²]	Jc_cab at 15T, 4.2K [A/mm ²]
CR4	1.25	24	1.25	15.6	2.175	0.2	666.67	428.9

The notches 1, 2 and 3 have respectively 38, 27 and 16 conductors; their angles are 12, 36 and 60 degrees.

The iron yoke thickness is 350 mm. The outer cylinder is 28 mm thick

4.4.1 Magnetic aspects of a 88 mm slot design dipole

Central field at 4.2 K[T]	I [A]	b1 -	b3 -	b5 -	b7 -	L [mH/m]	Em [kJ/m]	copper current density [A/mm ²]
13.76	16905	10000	-24.045	-0.041	0.020	13.28	1897.8	1033.2

The reference radius for the multipole calculation is 10 mm.

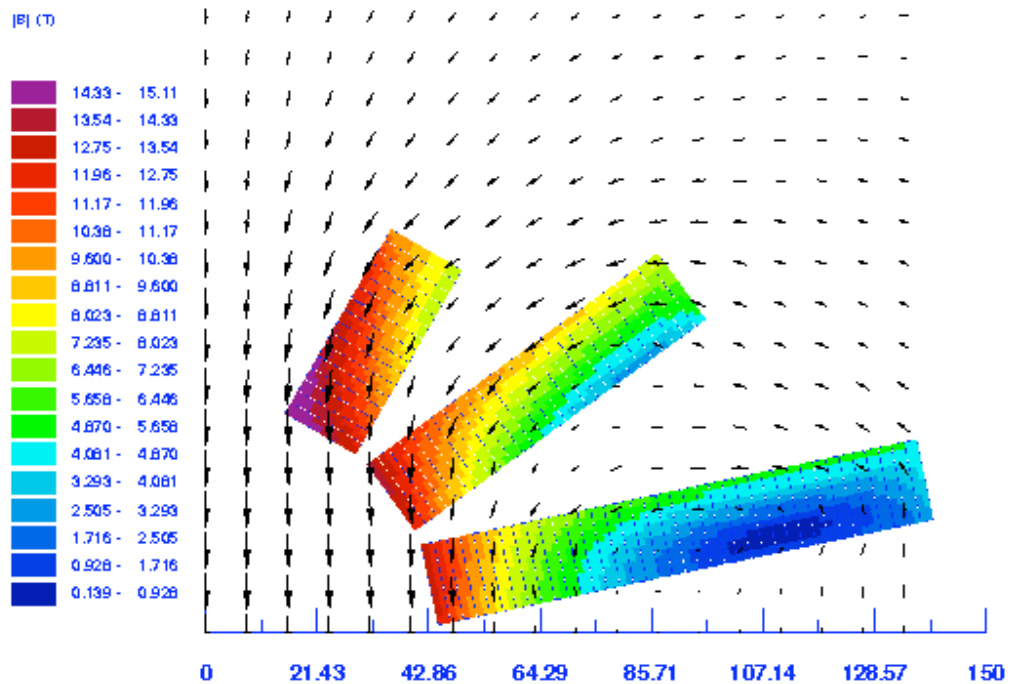


Fig. 22 Magnetic induction distribution (design CRT4_opt)

conductor number	Peak field [T]	% on load line [%]	Peak/Central [%]
1	13.27	89.54	96.4
39	13.71	92.03	99.6
66	15.12	100.01	109.8

Block 1, 39 and 66 are the inner most blocks of notches 1, 2 and 3.

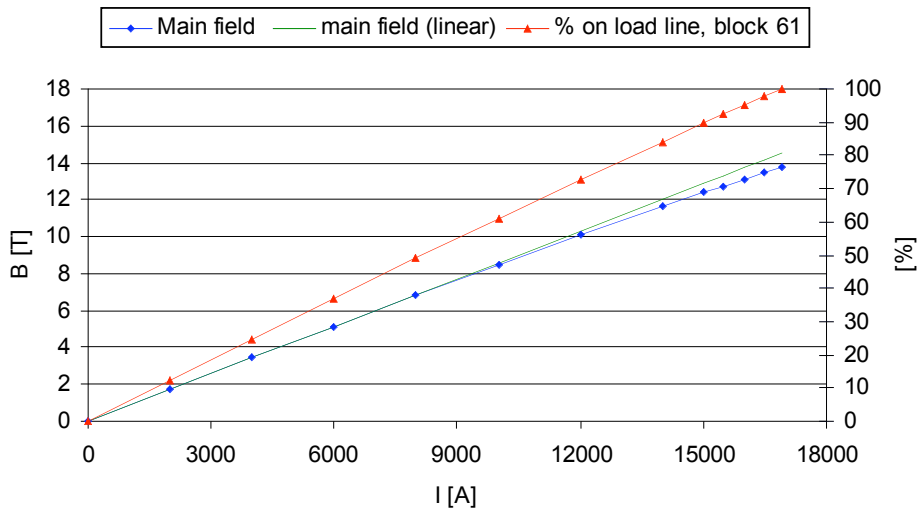


Fig. 23 Transfer function (design CRT4_opt)

The difference between the central field actually obtained in the magnet and the linear extrapolation of the low field load line is of 5.31 % at the quench field of 13.76 T in the bore.

4.4.2 Electro-magnetic forces aspects of a 88 mm slot design dipole

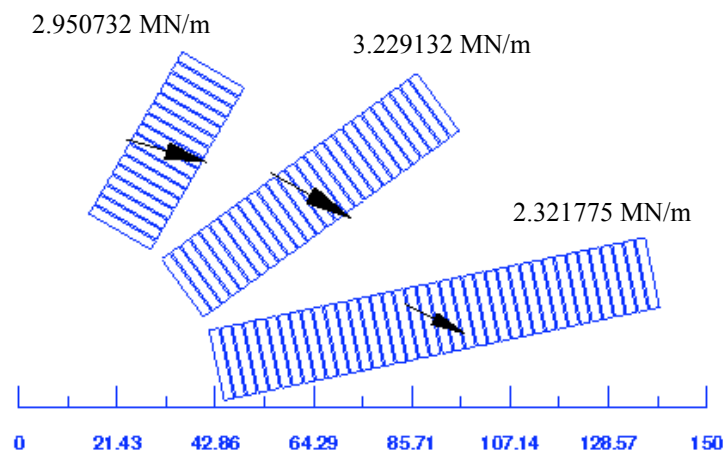


Fig. 24 Magnetic forces (design CRT4_opt) -(Only the 3rd digit is significant).

Notch	P+ [MPa]	P- [MPa]	P -azi [MPa]	Sum Fx [Tonnes/m]	F_notch [MN/m]
1	135.30	-17.59	-14.53	418.42	1.836258
2	97.02	-10.22	-42.19	563.76	1.353955
3	49.48	-3.15	-69.41	568.19	0.722792
				1550.37	

Below (Fig. 25) is shown the distribution of the azimuthal pressure acting on each conductor of each notch, with respect to the average pressure for the whole notch.

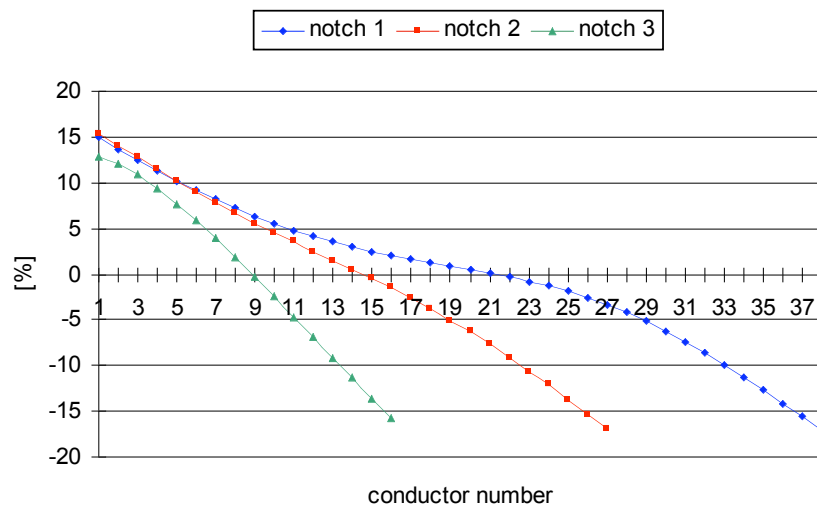


Fig. 25 Azimuthal pressure distribution (with respect to the average value for the notch) (design CRT4_opt)

For notches 1, 2, 3 the average azimuthal pressures are respectively -17.20 MPa, -49.95 MPa and -82.18 MPa.

(Here the insulation surface is not taken into account for the pressure calculation).

The shear stress between two adjacent conductors in a notch is given by the difference between the azimuthal components of the forces acting on the two blocks, and divided by the height of the cable.

The distribution of the shear stresses between conductors is shown in Fig. 26.

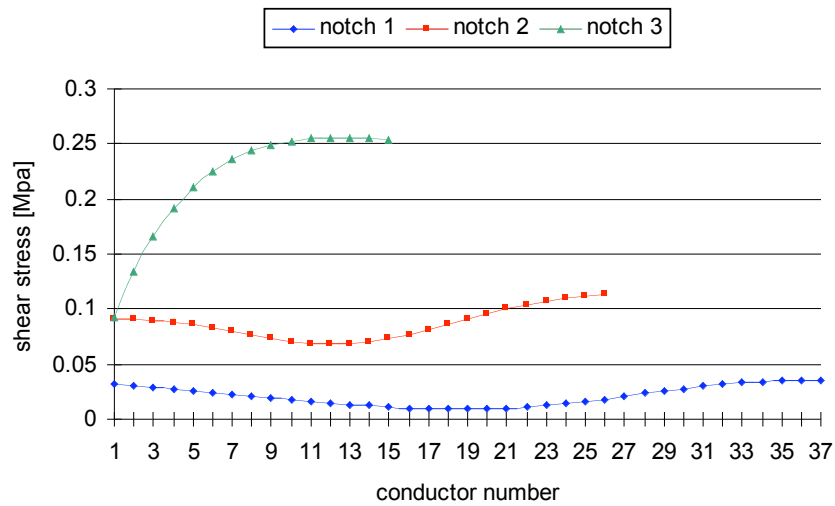


Fig. 26 Shear stress distribution (design CRT4_opt)

The shear stresses, acting mainly on the insulation, are acceptable.

4.4.3 Conductor Losses of a 88 mm slot design dipole

4.4.3.1 Hysteretic losses

For the cable used in design CRT4_opt, we have:

d_f [μm]	h [mm]	w [mm]	Cu/non_Cu -
50	15.6	2.175	1.25

Taking the parameterisation described in Annex 1 for the superconductor critical density and assuming a cycle from 0.01 to 14 T and back to 0.01 T, we get for the whole magnet:

$$Q_{\text{hyst}} = 15946 \text{ J/m/cycle}$$

4.4.3.2 Inter-filament losses

Cu/non_Cu -	$L_{p,f}$ [mm]	ρ_{eff} [$\Omega\cdot\text{m}$]	RRR -
1.25	30	6.80E-11	250

Here $\rho_{\text{eff}} = \rho_{\text{matrix}}$: we assume that half of the filaments contribute to the transverse resistivity of the matrix.

The ramp rate for the magnetic field increase is 0.1 T/s.

We then get:

$$P_{\text{if}} = 10.67 \text{ W/m}$$

$$\tau_{\text{if}} = 211 \text{ ms (time constant of the inter-filaments coupling currents)}$$

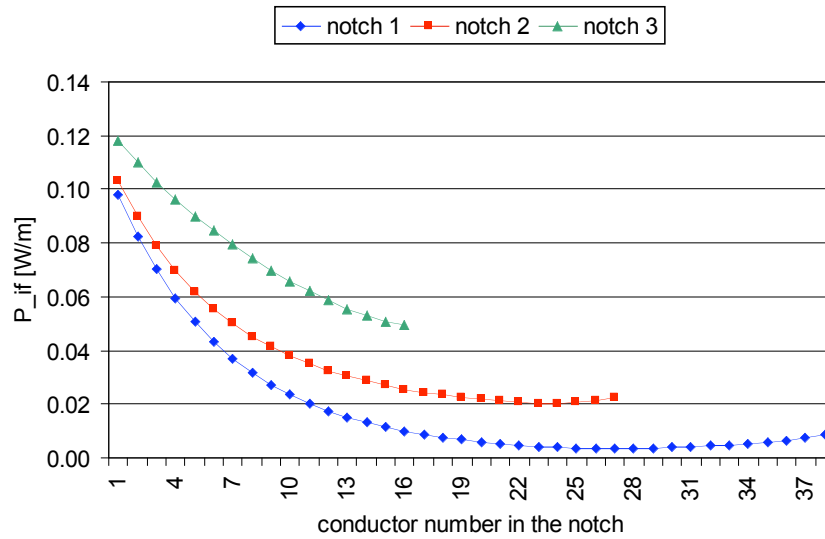


Fig. 27 Inter-filament coupling losses in each conductor (design CRT4_opt)

4.4.3.3 Inter-strands coupling losses:

The ramp rate for the magnetic field increase is 0.1 T/s.

$L_{p,s}$ [mm]	h [mm]	w [mm]	strand number -	R_a [μohm]	R_c [μohm]	P_a [W/m]	P_c [W/m]
110	15.6	2.175	24	1000	100	0.002	0.681
				1	100	2.392	0.681

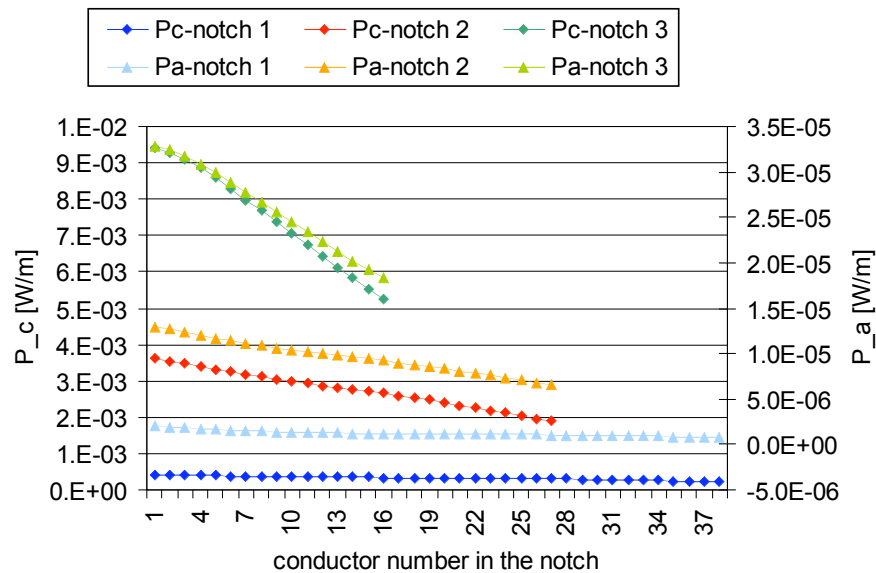


Fig. 28 Inter-strands losses in each conductor of the 3 notches for $R_a = 1000\mu\Omega$ and $R_c = 100 \mu\Omega$ At a ramp rate of 0.1 T/s (design CRT4_opt)

4.4.4 Overall Characteristics of the 88 mm, base line slot design

Layer design: rectangular cable

Cable: 24x1.25 mm ϕ

Field [T] / Current [A]	L [mH/m]	E/m [kJ/m]	Max pressure [MPa]	F _x , result. [MN/m]	P _c - 100 $\mu\Omega$ - 0.1T/s [W/m]	P _a - 1 $\mu\Omega$ - 0.1T/s [W/m]	Overall diameter [mm]
13.7 / 16900	13.3	1900	135	15.5	0.7	2.4	1090

4.5 Base line designs for a slot type dipole of 130 mm aperture

The cable used is CR4:

cable name	strand diam. [mm]	strand number	Cu/ non_Cu	height [mm]	width [mm]	insulation [mm]	J _c _str at 15T, 4.2K [A/mm ²]	J _c _cab at 15T, 4.2K [A/mm ²]
CR4	1.25	24	1.25	15.6	2.175	0.2	666.67	428.9

We now have 4 notches per quadrant in the structure. The notches 1, 2, 3 and 4 have respectively 40, 32, 22 and 14 conductors; their angles are 9, 25, 41 and 57 degrees.
The iron yoke inner radius is 193 mm and its thickness is 500mm.
The outer cylinder is 37 mm thick.

4.5.1 Magnetic aspects of a 130 mm slot design dipole

Central field [T]	I [A]	b1 -	b3 -	b5 -	b7 -	L [mH/m]	E/m [kJ/m]	copper current density [A/mm ²]
14.03	15825	10000	0.863	-0.223	0.003	27.15	3439.0	967.15

The reference radius for the multipole calculation is 10 mm.

Block number	Peak field [T]	% on load line [%]	Peak/Central [%]
1	13.84	91.84	98.6
41	14.08	93.20	100.3
73	14.43	95.17	102.8
95	15.28	100.00	108.9

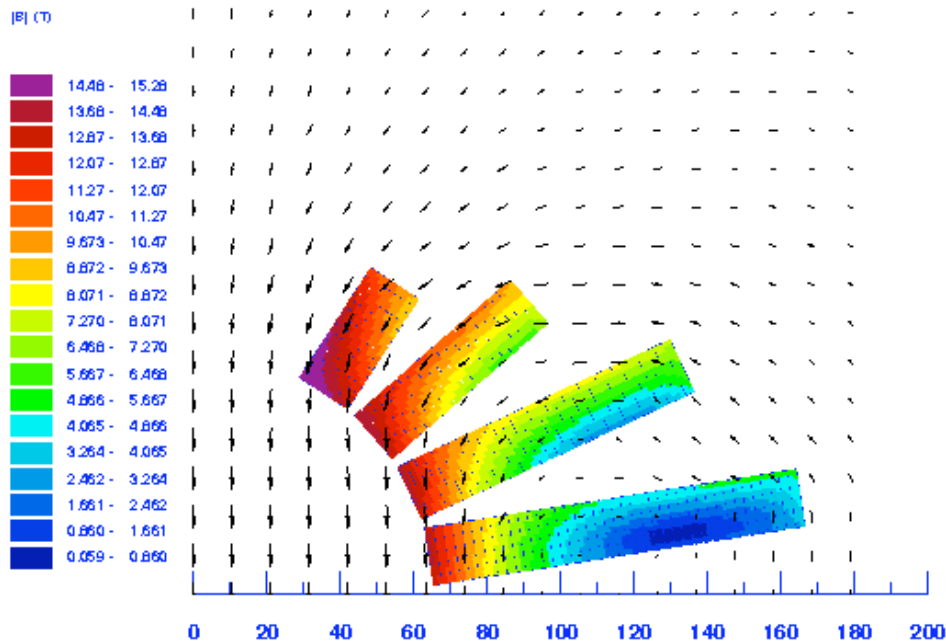


Fig. 29 Magnetic induction distribution (design CRT9)

4.5.2 Electro-magnetic force aspects of a130 mm slot design dipole

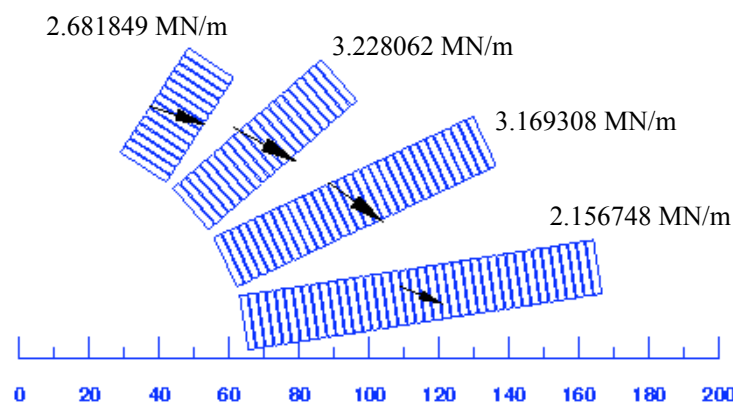


Fig. 30 Magnetic forces on conductors (design CRT9) -(Only the 3rd digit is significant).

notch	P+ [MPa]	P- [MPa]	P -azi [MPa]	Sum Fx [MN/m]	F_notch [MN/m]
1	140.44	-23.11	-11.10	4.16	1.830294
2	115.86	-16.29	-33.54	5.16	1.553256
3	79.49	-6.89	-53.35	5.68	1.13269
4	44.96	-1.65	-71.97	5.09	0.67558
				20.09	

Below is shown the distribution of the azimuthal pressure acting on each conductor of each notch, with respect to the average pressure for the whole notch:

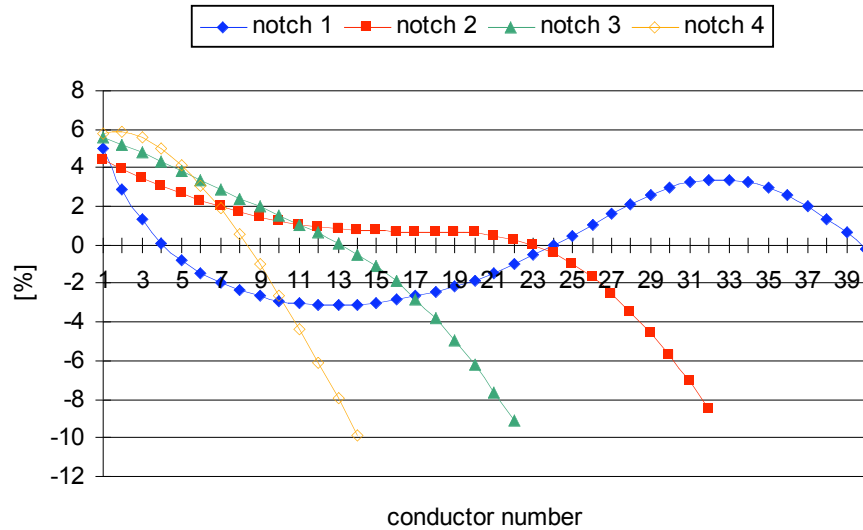


Fig. 31 Azimuthal pressure distribution (with respect to the average value for the notch) (design CRT9)

For notches 1, 2, 3 and 4 the average azimuthal pressures are respectively: -13.14 MPa, -39.71 MPa, -63.16 MPa and -85.20 MPa. (Here the insulation surface is not taken into account for the pressure calculation).

The shear stresses between conductors are presented in Fig 32.

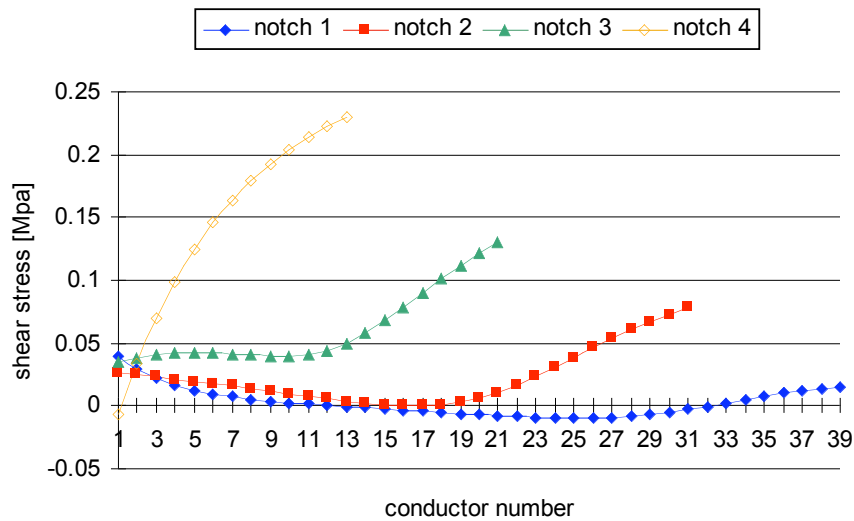


Fig. 32. Shear pressure distribution (design CRT9)

4.5.3 Conductor Losses in a 130 mm slot design dipole

4.5.3.1 Hysteretic losses

For the cable used in design CRT9, we have:

d_f [μm]	h [mm]	w [mm]	Cu/non_Cu
50	15.6	2.175	1.25

Taking the parameterisation described in Annex 1 for the superconductor critical density and assuming a cycle from 0.01 to 14 T and back to 0.01 T, we get for the whole magnet:

$$Q_{\text{hyst}} = 21261 \text{ J/m/cycle}$$

For 50 cycles from 11 T to 11.5 T and back to 11T, we get for the whole magnet:

$$Q_{\text{hyst}} = 10076 \text{ J/m}$$

4.5.3.2 Inter-filament losses

Cu/non_Cu	$L_{p,f}$ [mm]	ρ_{eff} [$\Omega \cdot \text{m}$]	RRR
-	30	$6.80\text{E-}11$	-
1.25			250

Here $\rho_{\text{eff}} = \rho_{\text{matrix}}$: we assume that half of the filaments contribute to the transverse resistivity of the matrix.

For a ramp rate for the field increase of 0.1 and 0.5 T/s we get respectively:

$$P_{\text{if}} = 17.57 \text{ W/m and } 439.37 \text{ W/m}$$

$$\tau_{\text{if}} = 211 \text{ ms (time constant of the inter-filaments coupling currents)}$$

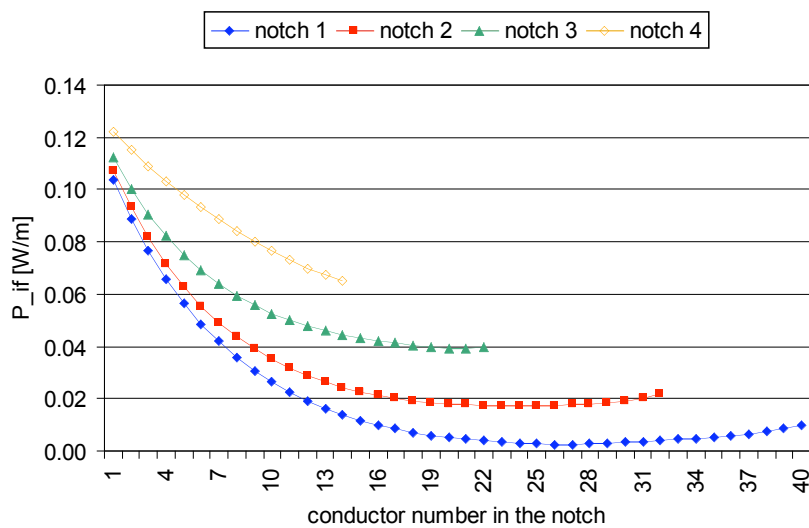


Fig. 33 Inter-filaments losses in each conductor of the 4 notches (field ramp rate of 0.1 T/s) (design CRT9)

4.5.3.3 Inter-strands coupling losses

For a ramp rate for the magnetic field increase of 0.1 T/s we have for the whole magnet:

Lp,s [mm]	h [mm]	w [mm]	strand number	Ra [μohm]	Rc [μohm]	P_a [W/m]	P_c [W/m]
110	15.6	2.175	24	1000	100	0.004	1.189
				1	100	4.173	1.189

And for a ramp rate for the magnetic field increase of 0.5 T/s we have:

Lp,s [mm]	h [mm]	w [mm]	strand number	Ra [μohm]	Rc [μohm]	P_a [W/m]	P_c [W/m]
110	15.6	2.175	24	1000	100	0.104	29.736
				1	100	104.32	29.736

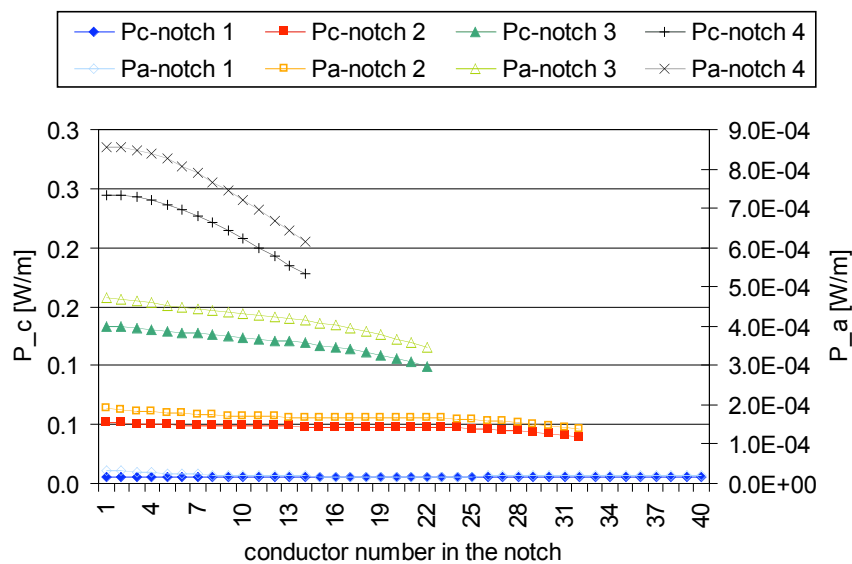


Fig. 34 Inter-strands losses for each conductor (for a field ramp rate of 0.5 T/s and Ra = 1000 μΩ, Rc = 100 μΩ) (design CRT9)

4.5.4 Another design, with larger cable, of a 130 mm slot type dipole

It appears that using a cable of 24 strands leads to a rather high value of self-inductance, which can make the protection in case of a quench more difficult. Using a larger cable will reduce the self-inductance.

The cable used is now CR7:

cable name	strand diam. [mm]	strand number	Cu/non_Cu	height [mm]	width [mm]	insulation [mm]	Jc_str at 15T, 4.2K [A/mm ²]	Jc_cab at 15T, 4.2K [A/mm ²]
CR7	1.25	32	1.25	20.8	2.175	0.2	666.67	431.62

We now have only 3 notches per quadrant in the structure.

The notches 1, 2, and 3 have respectively 39, 27 and 15 conductors; their angles are 9, 25 and 41 degrees.

The iron yoke inner radius is 191 mm and its thickness is 500mm. The outer cylinder is 37 mm thick. This gives the following magnetic field distribution:

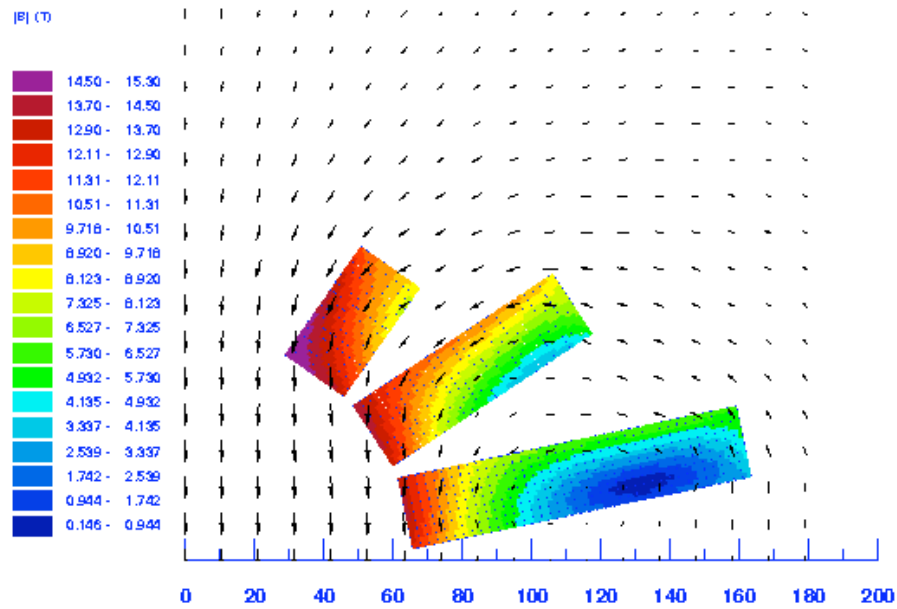


Fig. 35. Magnetic field distribution of a 130 mm slot design (design CRT9_31)

Central field [T]	I [A]	b1 -	b3 -	b5 -	b7 -	L [mH/m]	E/m [kJ/m]	copper current density [A/mm ²]
13.92	21000	10000	-1.192	-0.217	0.003	15.22	3356.25	962.57

The reference radius for the multipole calculation is 10 mm.

conductor number	Peak field [T]	% on load line [%]	Peak/Central [%]
1	13.85	91.85	99.5
40	14.24	94.04	102.3
67	15.30	100.05	109.9

The electromagnetic forces in the structure are:

P+ [MPa]	P- [MPa]	P -azi [MPa]	Sum Fx [MN/m]	F_notch [MN/m]
139.02	-21.87	-19.36	5.58	2.436738
98.82	-11.85	-56.99	7.40	1.809121
50.04	-2.37	-89.87	6.82	0.991691
			19.80	

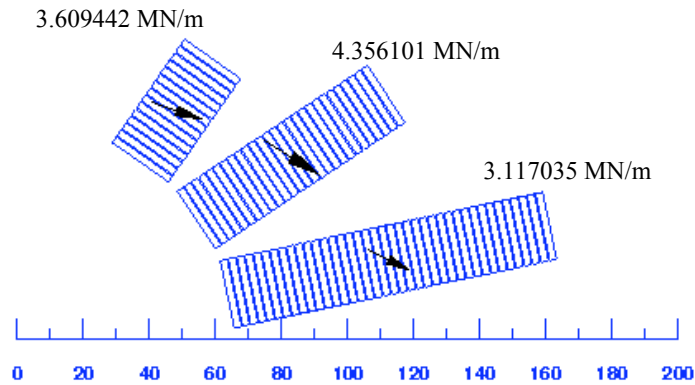


Fig. 36. Magnetic forces distribution (design CRT9_31) -(Only the 3rd digit is significant).

Below is shown the distribution of the azimuthal pressure acting on each conductor of each notch, with respect to the average pressure for the whole notch:

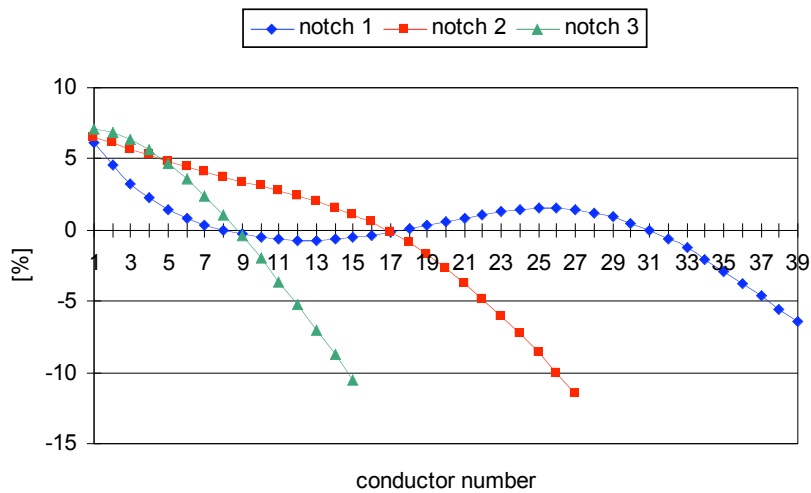


Fig. 37. Azimuthal pressure distribution (with respect to the average value for the notch) (design CRT9_31)

For notches 1, 2 and 3 the average azimuthal pressures are respectively: -22.92 Mpa, -67.47 Mpa, and -106.40 Mpa. (Here the insulation surface is not taken into account for the pressure calculation).

The shear stresses between conductors are presented in Fig 38.

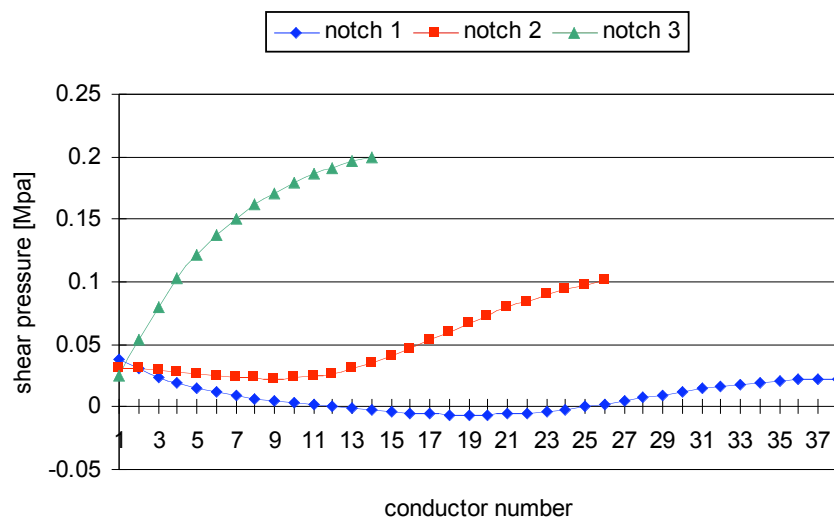


Fig. 38 Shear stress distribution (design CRT9_31)

For the calculations of the conductor losses, we assume the following parameters for the cable and strands:

d_f [μm]	$L_{p,f}$ [mm]	$L_{p,s}$ [mm]	Cu/non Cu -	ρ_{eff} [$\Omega\cdot\text{m}$]	RRR -
50	30	146	1.25	6.80 E-11	250

This then gives:

Hysteretic losses:

field cycle [T]	number of cycle -	Q_{hyst} [J/m]
0.01 -> 14 -> 0.01	1	21261.5
11 -> 11.5 -> 11	50	10076.1

Inter-filament coupling losses:

τ_{if} [ms]	field ramp rate [T/s]	P_{if} [W/m]
211	0.1	17.63
211	0.5	440.69

Inter-strands coupling losses:

field ramp rate [T/s]	R_a [μohm]	R_c [μohm]	P_a [W/m]	P_c [W/m]
0.1	1000	100	0.727	3.696
0.1	1	100	7.266	3.696
0.5	1000	100	0.182	92.404
0.5	1	100	182.652	92.404

4.5.5 Comparison of the two 130 mm slot design CRT9 and CRT9_31

name	cable name	number of notches	notches angles [deg]	number of conductors	iron yoke inner radius [mm]	iron yoke thickness [mm]	overall radius [mm]
CRT9	CR4	4	9, 25, 41, 57	40, 32, 22, 14	193	500	718
CRT9_31	CR7	3	9, 25, 41	39, 27, 15	191	500	716

cable name	strand diam. [mm]	strand number	Cu/non_Cu	height [mm]	width [mm]	isolation [mm]	Jc_str at 15T, 4.2K [A/mm ²]	Jc_cab at 15T, 4.2K [A/mm ²]
CR4	1.25	24	1.25	15.6	2.175	0.2	666.67	428.9
CR7	1.25	32	1.25	20.8	2.175	0.2	666.67	431.62

name	Central field [T]	current [A]	L [mH/m]	E/m [kJ/m]	copper current density [A/mm ²]	P_if (0.1T/s) [W/m]	P_c (Rc = 100mΩ, 01T/s) [W/m]
CRT9	14.03	15825	27.15	3438.99	967.15	17.575	1.189
CRT9_31	13.92	21000	15.22	3356.25	962.57	17.627	3.696

name	P+ max [MPa]	P- max [MPa]	P -azi max [MPa]	Sum Fx total [MN/m]	F_notch max [MN/m]
CRT9	140.44	-23.11	-71.97	20.09	1.830294
CRT9_31	139.02	-21.87	-89.87	19.8	2.436738

4.6 Base line designs for a slot type dipole of 160 mm aperture

The cable used is CR4:

cable name	strand diam. [mm]	strand number	Cu/non_Cu	height [mm]	width [mm]	insulation [mm]	Jc_str at 15T, 4.2K [A/mm ²]	Jc_cab at 15T, 4.2K [A/mm ²]
CR4	1.25	24	1.25	15.6	2.175	0.2	666.67	428.9

We now have 5 notches per quadrant in the structure.

The blocks 1, 2, 3, 4 and 5 have respectively 38, 33, 25, 18 and 12 conductors; their angles are 8, 21.5, 35, 48.5 and 62 degrees.

The iron yoke inner radius is 203 mm and its thickness is 500mm. The outer cylinder is 44 mm thick.

4.6.1 Magnetic aspects of a 160 mm slot design dipole

Central field [T]	I [A]	b1 -	b3 -	b5 -	b7 -	L [mH/m]	E/m [kJ/m]	copper current density [A/mm ²]
13.97	15420	10000	-1.518	-0.074	0.001	37.37	4443.4	942.4

The reference radius for the multipole calculation is 10 mm.

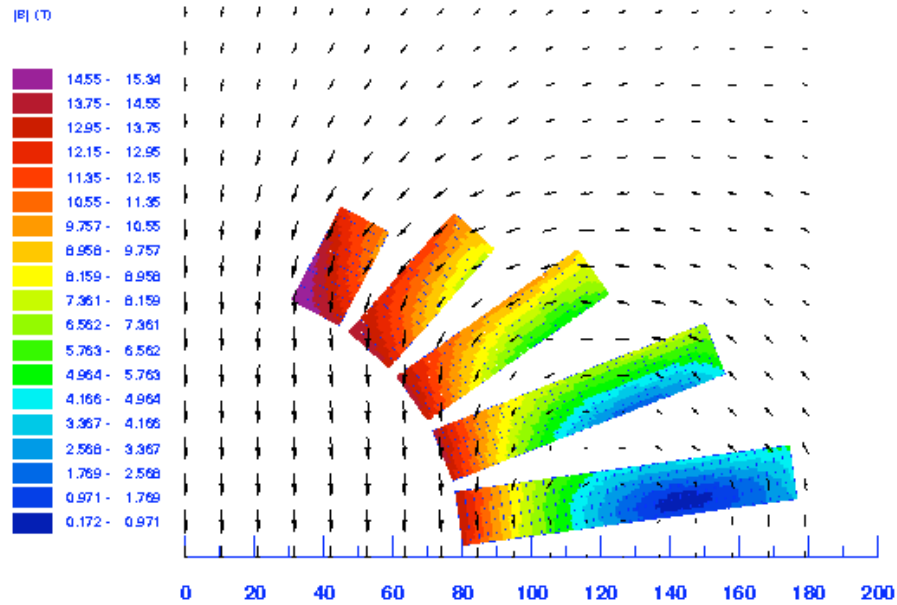


Fig. 39. Magnetic induction distribution (design CRT14)

conductor number	Peak field [T]	% on load line [%]	Peak/Central [%]
1	13.70	90.71	98.1
39	13.92	91.97	99.7
72	14.11	93.05	101.0
97	14.46	95.02	103.5
115	15.35	100.03	109.9

4.6.2 Electro-magnetic force aspects of a 160 mm slot design dipole

notch	P+ [MPa]	P- [MPa]	P -azi [MPa]	Sum Fx [MN/m]	F_notch [MN/m]
1	135.34	-22.56	-8.95	3.73	1.759409
2	117.44	-19.82	-28.51	4.62	1.522868
3	88.64	-11.20	-45.42	5.34	1.208090
4	58.71	-5.18	-60.13	5.29	0.835132
5	32.75	-1.42	-74.34	4.52	0.488760
				23.50	

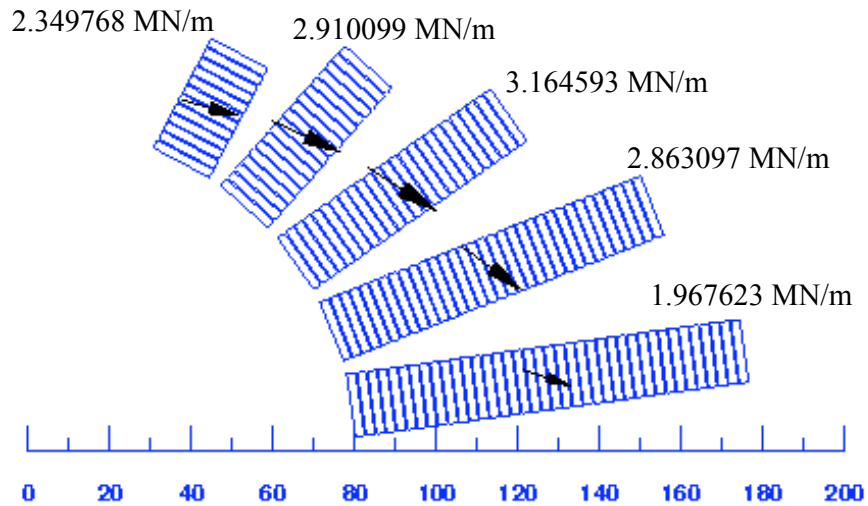


Fig. 40. Magnetic forces on conductors (design CRT14) -(Only the 3rd digit is significant).

Below is shown the distribution of the azimuthal pressure acting on each conductor of each notch, with respect to the average pressure for the whole notch.

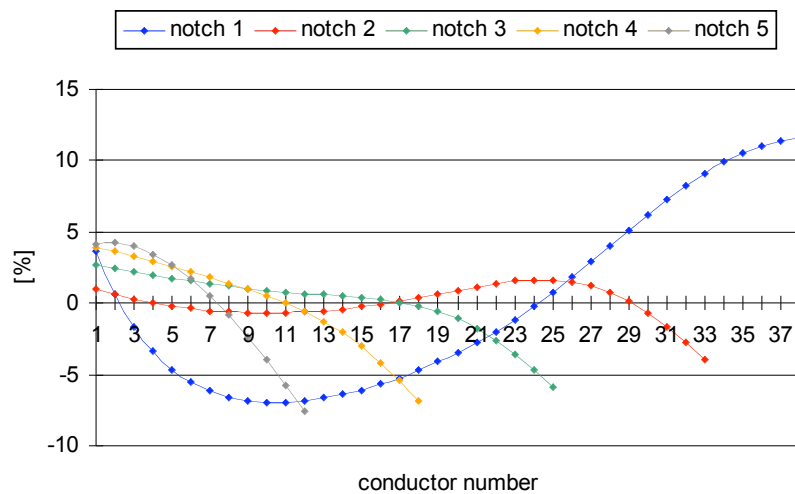


Fig. 41 Azimuthal pressure distribution (with respect to the average value for the notch) (design CRT14)

For notches 1, 2, 3, 4 and 5; the average azimuthal pressures are respectively: -10.59 MPa, -33.76 MPa, -53.78 MPa, -71.19 MPa and -88.02 MPa.

The shear stresses between conductors are presented in Fig. 42.

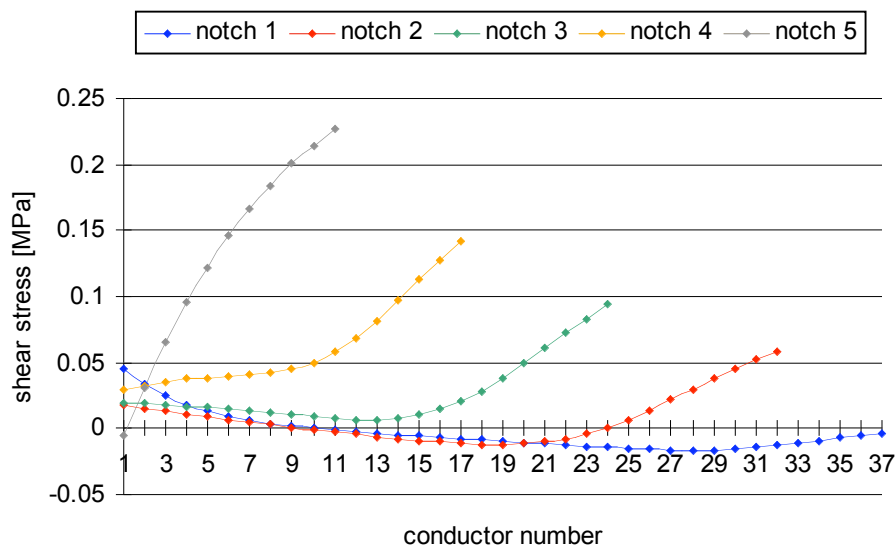


Fig. 42 Shear stress distribution (design CRT14)

4.6.3 Conductor Losses in a 160 mm slot design dipole

4.6.3.1 Hysteretic losses

For the cable used in design CRT14, we have:

d_f [μm]	h [mm]	w [mm]	Cu/non_Cu -
50	15.6	2.175	1.25

Taking the parameterisation described in Annex 1 for the superconductor critical density and assuming a cycle from 0.01 to 14 T and back to 0.01 T, we get for the whole magnet:

$$Q_{\text{hyst}} = 24804 \text{ J/m/cycle}$$

For 50 cycles from 11 T to 11.5 T and back to 11T, we get for the whole magnet:

$$Q_{\text{hyst}} = 11755 \text{ J/m}$$

4.6.3.2 Inter-filament losses

Cu/non_Cu -	$L_{p,f}$ [mm]	ρ_{eff} [$\Omega\cdot\text{m}$]	RRR -
1.25	30	6.80E-11	250

Here $\rho_{\text{eff}} = \rho_{\text{matrix}}$: we assume that half of the filaments contribute to the transverse resistivity of the matrix.

For a ramp rate for the field increase of 0.1 and 0.5 T/s we get respectively:

$$P_{\text{if}} = 21.87 \text{ W/m and } 546.85 \text{ W/m}$$

$$\tau_{\text{if}} = 211 \text{ ms (time constant of the inter-filaments coupling currents)}$$

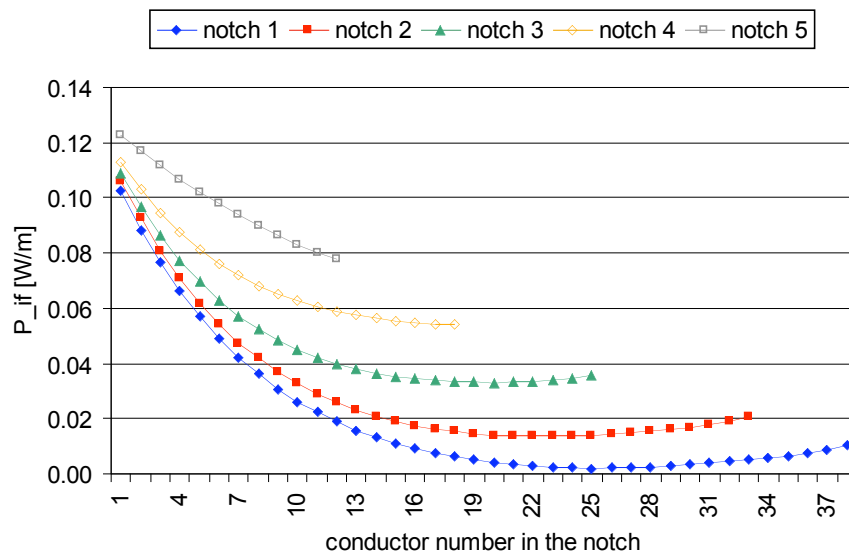


Fig. 43. Inter-filaments losses in each conductor of the 5 notches (field ramp rate of 0.1 T/s) (design CRT14)

4.6.3.3 Inter-strand coupling losses

For a ramp rate for the magnetic field increase of 0.1 T/s, we have for the whole magnet:

$L_{p,s}$ [mm]	h [mm]	w [mm]	strand number -	R_a [μohm]	R_c [μohm]	P_a [W/m]	P_c [W/m]
110	15.6	2.175	24	1000	100	0.005	1.526
				1	100	5.350	1.526

And for a ramp rate for the magnetic field increase of 0.5 T/s we have:

$L_{p,s}$ [mm]	h [mm]	$\langle w \rangle$ [mm]	strand number -	R_a [μohm]	R_c [μohm]	P_a [W/m]	P_c [W/m]
110	15.6	2.175	24	1000	100	0.133	38.154
				1	100	133.759	38.154

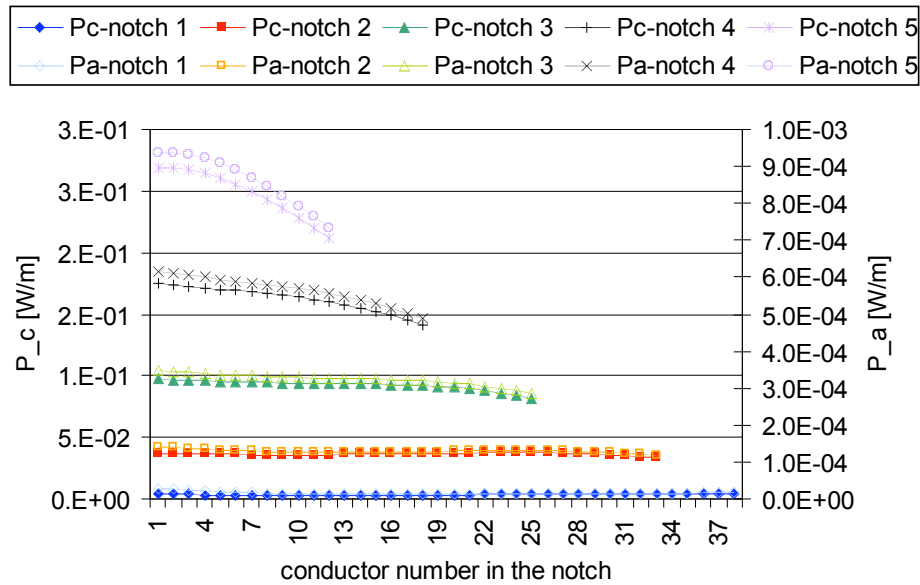


Fig. 44. Inter-strands losses for each conductor (for a field ramp rate of 0.5 T/s and $R_a = 1000 \mu\Omega$, $R_c = 100 \mu\Omega$) (design CRT14)

4.6.4 Another design, with larger cable, of a 160 mm slot type dipole

The cable used is now CR7:

cable name	strand diam. [mm]	strand number	Cu/non_Cu	height [mm]	width [mm]	insulation [mm]	Jc_str at 15T, 4.2K [A/mm ²]	Jc_cab at 15T, 4.2K [A/mm ²]
CR7	1.25	32	1.25	20.8	2.175	0.2	666.67	431.62

We now have only 4 notches per quadrant in the structure.

The notches 1, 2, 3 and 4 have respectively 30, 23, 14 and 8 conductors; their angles are 9.5, 26.5, 43.5 and 60.5 degrees.

The iron yoke inner radius is 183 mm and its thickness is 640mm.

This gives the following magnetic field distribution:

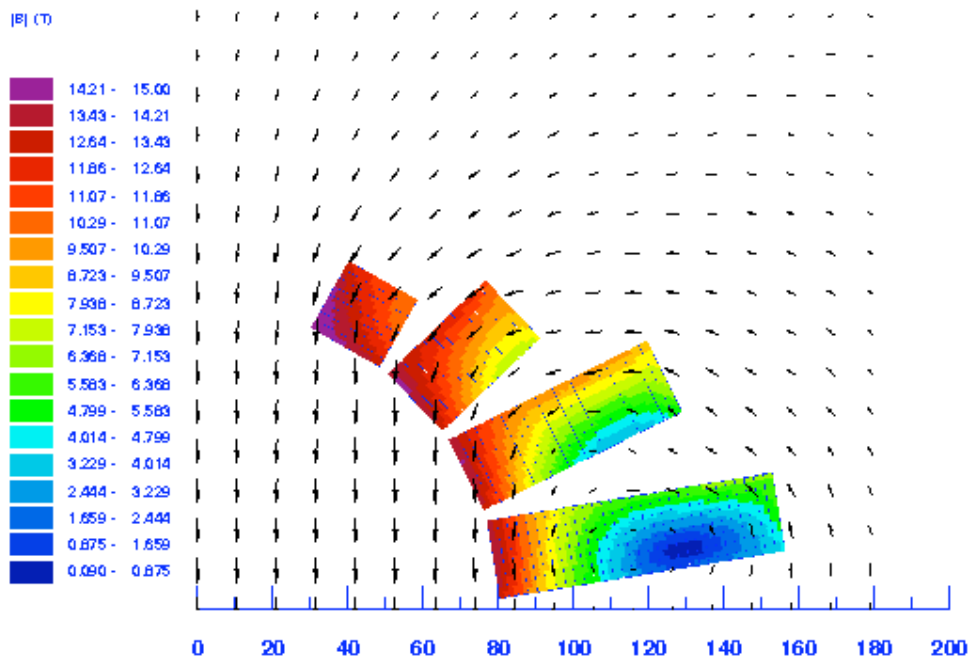


Fig. 45. Magnetic field distribution of a 160 mm slot design (design CRT14_31)

Central field at 4.2 k [T]	I [A]	b1 -	b3 -	b5 -	b7 -	L [mH/m]	E/m [kJ/m]	copper current density [A/mm ²]
13.87	23670	10000	3.935	-0.079	0.001	14.13	3958.78	1084.95

The reference radius for the multipole calculation is 10 mm.

Block number	Peak field [T]	% on load line [%]	Peak/central [%]
1	14.11	95.03	101.7
31	14.22	95.68	102.5
54	14.25	95.85	102.8
69	15.00	100.08	108.2

The electromagnetic forces in the structure are:

Block	P+ [MPa]	P- [MPa]	P -azi [MPa]	Sum Fx [MN/m]	F_notch [MN/m]
1	128.77	-25.92	-19.94	4.73	2.139464
2	98.45	-16.43	-59.44	6.21	1.705936
3	57.03	-4.83	-89.37	6.02	1.085730
4	25.29	-0.90	-111.69	4.51	0.507338
				21.48	

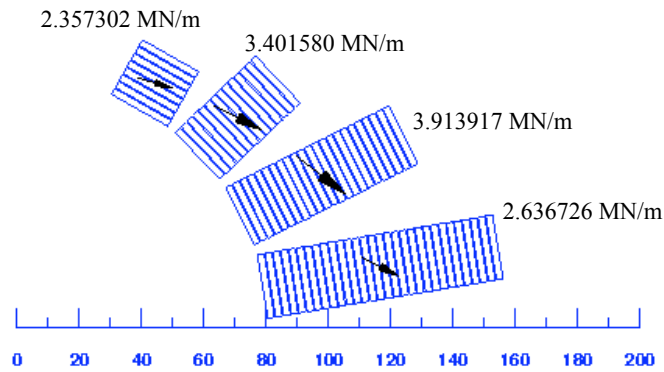


Fig. 46. Magnetic forces distribution (design CRT14_31) -(Only the 3rd digit is significant).

Below is shown the distribution of the azimuthal pressure acting on each conductor of each notch, with respect to the average pressure for the whole notch:

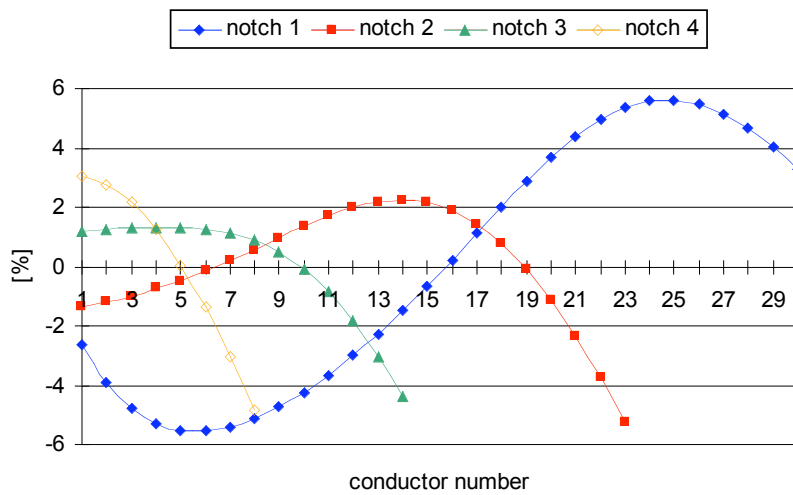


Fig.47. Azimuthal pressure distribution (with respect to the average value for the notch) (design CRT14_31)

For notches 1, 2, 3 and 4 the average azimuthal pressures are respectively: -23.61 Mpa, -70.38 Mpa, -105.81 Mpa and -132.23 Mpa.

(Here the insulation surface is not taken into account for the pressure calculation).

The shear stresses between conductors are presented in Fig. 48.

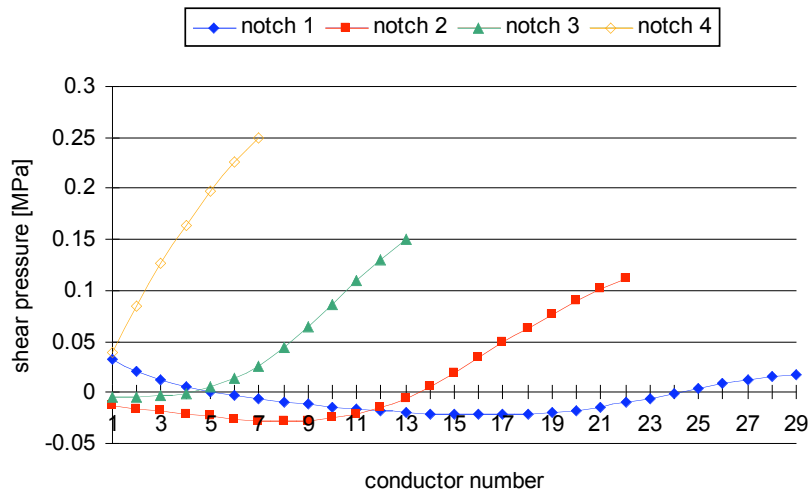


Fig. 48. Shear stress distribution (design CRT14_31)

For the calculations of the conductor losses, we assume the following parameters for the cable and strands:

d_f [μm]	$L_{p,f}$ [mm]	$L_{p,s}$ [mm]	Cu/non Cu	ρ_{eff} [$\Omega\cdot\text{m}$]	RRR
50	30	146	-	6.80E-11	-
			1.25		250

This then gives:

Hysteretic losses:

field cycle [T]	number of cycle	Q_{hyst} [J/m]
0.01 -> 14 -> 0.01	1	19686.61
11 -> 11.5 -> 11	50	9329.7

Inter-filament coupling losses:

τ_{if} [ms]	field ramp rate [T/s]	P_{if} [W/m]
211	0.1	18.56
211	0.5	463.9

Inter-strands coupling losses:

field ramp rate [T/s]	R_a [μohm]	R_c [μohm]	P_a [W/m]	P_c [W/m]
0.1	1000	100	0.008	3.988
0.1	1	100	7.837	3.988
0.5	1000	100	0.196	99.700
0.5	1	100	195.937	99.700

4.6.5 Comparison of the two 160 mm slot design CRT14 and CRT14_31

name	cable name	number of notches	notches angles [deg]	number of conductors	iron yoke inner radius [mm]	iron yoke thickness [mm]	overall radius [mm]
CRT14	CR4	5	8, 21.5, 35, 48.5, 62	38, 33, 25, 18, 12	203	640	868
CRT14_31	CR7	4	9.5, 26.5, 43.5, 60.5	30, 23, 14, 8	183	640	848

cable name	strand diam. [mm]	strand number	Cu/non_Cu	height [mm]	width [mm]	insulation [mm]	Jc_str at 15T, 4.2K [A/mm ²]	Jc_cab at 15T, 4.2K [A/mm ²]
CR4	1.25	24	1.25	15.6	2.175	0.2	666.67	428.9
CR7	1.25	32	1.25	20.8	2.175	0.2	666.67	431.62

name	Central field [T]	current [A]	L [mH/m]	E/m [kJ/m]	copper current density [A/mm ²]	P_if (0.1T/s) [W/m]	P_c (Rc = 100mΩ, 01T/s) [W/m]
CRT14	13.97	15420	37.37	4443.37	942.4	21.874	1.526
CRT14_31	13.87	23670	14.13	3958.78	1084.95	18.556	3.988

name	P+ max [MPa]	P- max [MPa]	P -azi max [MPa]	Sum Fx total [MN/m]	F_notch max [MN/m]
CRT14	135.34	-22.56	-74.34	23.50	1.759409
CRT14_31	128.77	-25.92	-111.69	21.47	2.139464

5. COMPARISON OF SLOT AND LAYER DESIGNS AS A FUNCTION OF APERTURE

The cables used in the various designs investigated are:

cable name	strand diam. [mm]	strand number	Cu/non_Cu	height [mm]	width [mm]	insulation [mm]	Jc_str at 15T, Jc_cab at	
							4.2K [A/mm ²]	15T, 4.2K [A/mm ²]
CK6	1.25	40	1.25	26	2.275	0.2	666.67	417.06
CR4	1.25	24	1.25	15.6	2.175	0.2	666.67	428.92
CR7	1.25	32	1.25	20.8	2.175	0.2	666.67	431.62

The cable CK6 is a keystone cable; the width reported above is the mid-width of the cable (the inner and outer width are respectively 2.175 and 2.375mm).

Geometrical dimensions for layer designs:

name	aperture [mm]	cable name	number of conductors	iron yoke inner radius [mm]	iron yoke thickness [mm]	overall radius [mm]
-	-	-	-	-	-	-
CK6_opt	88	CK6	45	124	350	502
CK11	130	CK6	62	145	500	682
CK16	160	CK6	76	160	640	844

Geometrical dimensions for slot designs:

name	aperture [mm]	cable name	number of notches	number of conductors	iron yoke inner radius [mm]	iron yoke thickness [mm]	overall radius [mm]
-	-	-	-	-	-	-	-
CRT4_opt	88	CR4	3	38, 27, 16	167	350	545
CRT9_31	130	CR7	3	39, 27, 15	191	500	728
CRT14_31	160	CR7	4	30, 23, 14, 8	183	640	867

Magnetic field aspects for layers designs:

name	aperture [mm]	central field [T]	current [A]	inductance [mH/m]	stored energy [kJ/m]	copper current density [A/mm ²]	peak field [T]
-	-	-	-	-	-	-	-
CK6_opt	88	14.42	28530	4.43	1803.67	1046.18	15.09
CK11	130	14.31	26310	8.71	3013.38	964.77	15.29
CK16	160	14.19	24810	13.18	4056.79	909.77	15.43

Magnetic field aspects for slot designs:

name -	aperture [mm]	Central field [T]	current [A]	inductance [mH/m]	stored energy [kJ/m]	copper current density [A/mm ²]	peak field on conduct. [T]
CRT4_opt	88	13.76	16905	13.28	1897.78	1033.16	15.12
CRT9_31	130	13.92	21000	15.22	3356.25	962.57	15.30
CRT14_31	160	13.87	23670	14.13	3958.78	1084.95	15.00

Electro-magnetic forces aspects for layer designs:

name -	aperture [mm]	Sum P -azi inner layer [MPa]	Sum P -azi outer layer [MPa]	Pressure Block 1 [MPa]	Sum Fx [MN/m]
CK6_opt	88	-147.830	-141.226	111.068	15.85
CK11	130	-214.871	-170.815	99.642	20.89
CK16	160	-252.126	-201.065	92.875	24.56

Electro-magnetic forces aspects for slot designs:

name -	aperture [mm]	maximum P + [MPa]	maximum P -azi [MPa]	maximum F notch [MN/m]	Sum Fx [Tonnes/m]
CRT4_opt	88	135.299	-69.41	1.836	15.5
CRT9_31	130	139.022	-89.87	2.437	19.8
CRT14_31	160	128.774	-111.69	2.139	21.5

Conductor losses aspects for layer designs:

name -	aperture [mm]	Q_hyst 0.01->14->0.01 T [J/m/cycle]	P_if at 0.1 T/s [W/m]	P_a Ra = 1μΩ, at 0.1T/s [W/m]	P_c Rc = 100μΩ, at 0.1T/s [W/m]
CK6_opt	88	15444	12.47	5.000	3.964
CK11	130	21278	18.67	6.818	9.011
CK16	160	26083	23.59	8.397	11.585

Conductor losses aspects for slot designs:

name -	aperture [mm]	Q_hyst 0.01->14->0.01 T [J/m/cycle]	P_if at 0.1T/s [W/m]	P_a Ra = 1mW, at 0.1T/s [W/m]	P_c Rc = 100mW, at 0.1T/s [W/m]
CRT4_opt	88	15946	10.67	2.392	0.681
CRT9_31	130	21261	17.63	7.266	3.696
CRT14_31	160	19686	18.56	7.837	3.988

6. MULTIPOLE OPTIMISATION IN THE SLOT DESIGN

The following paragraph shows that it is possible to optimize the multipole harmonics in the slot design by inserting spacers in the blocks.

The calculations are made for a 88mm dipole with a conductor of 20 strands (CR2) but the principle is valid for all the designs.

(It is the magnet called CRT2_315 in Annex IV).

cable name	total number of conductors	block angle [deg]	iron yoke internal radius [mm]
-	-	-	-
CR2	80	15, 40, 65	172

Central field at 4.2 K[T]	I [A]	b3 [10 ⁻⁴]	b5 [10 ⁻⁴]	b7 [10 ⁻⁴]	L [mH/m]	E/m [kJ/m]	copper current density [A/mm ²]
12.81	16470	-44.4571	0.2011	-0.0139	12.42	1684.05	1207.89

The following graphs show the variation of b3, b5 and b7 when a conductor is replaced by a dummy; the current is kept at 16470A in all other conductors.

The dummy number or dummy position (X-axis in Fig. 49, 50 and 51) is the position of the conductor in the notch, which is replaced by a dummy (conductor 1 is the closest conductor to the aperture).

b3 is influenced by dummy conductors in notches 1 and 3, (Fig. 49):

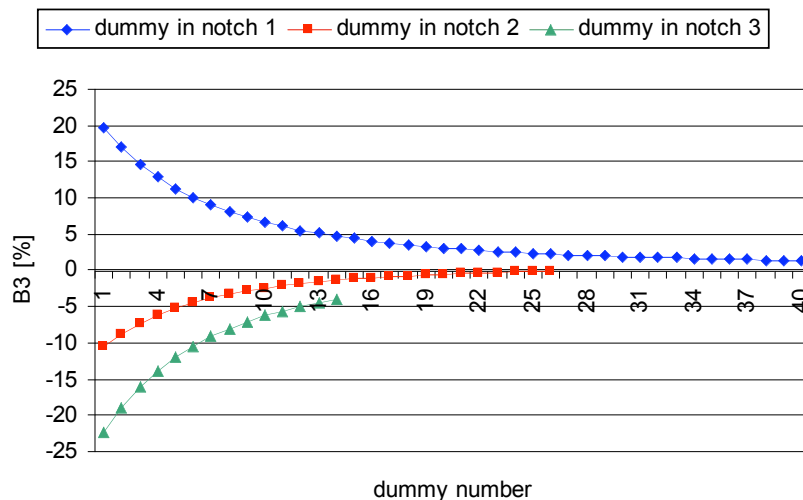


Fig. 49 Variation of b3 for dummy conductor in notches 1, 2 and 3

b5 is influenced by dummy conductors in notches 2 and 3, (Fig. 50):

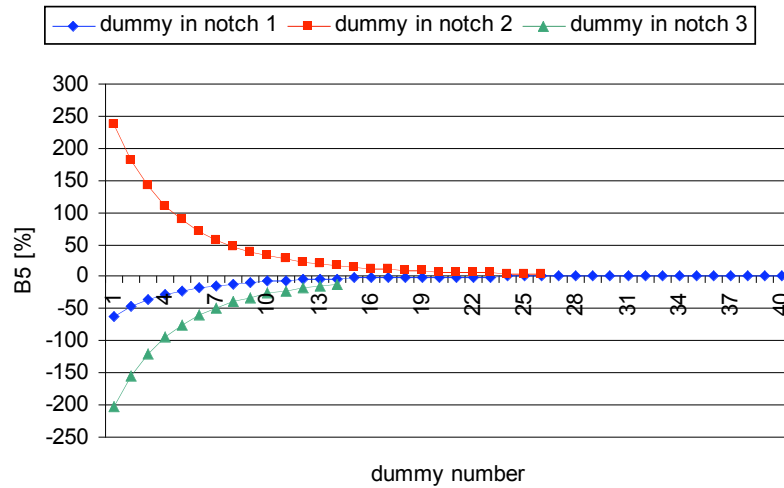


Fig. 50. Variation of b_5 for dummy conductor position in notches 1, 2 and 3

b_7 is influenced by dummy conductors in notches 1 and 2, (Fig. 51):

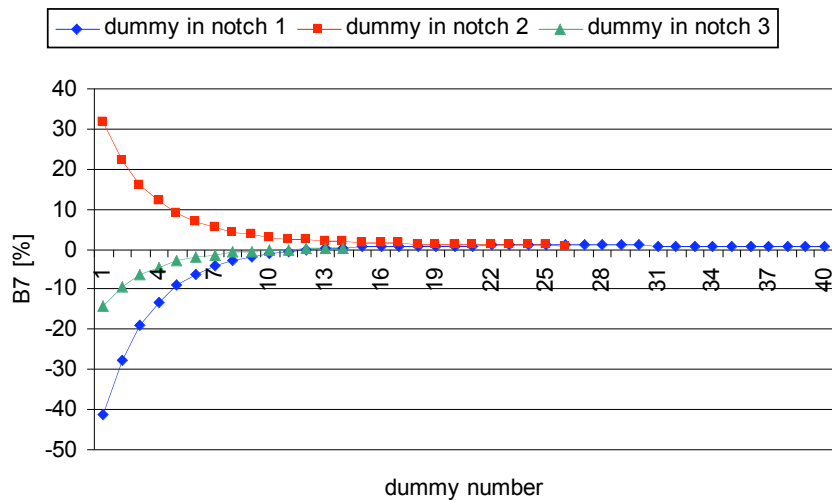


Fig. 51. Variation of b_7 for dummy conductor position in notches 1, 2 and 3

7. MULTIPOLE COMPENSATION AT LOW FIELD

The Nb₃Sn strands developed for high field magnets have a higher magnetisation due to a larger effective filament diameter (50 μm instead of 6 μm for NbTi).

It is possible to compensate this effect by introducing in the coils spacers made of ferromagnetic material.

The following graphs (Fig. 42 and 43) show the influence of replacing the copper wedge between to adjacent blocks by an iron wedge in the 88mm layer magnet (design CK6).

Five positions of the iron wedge are investigated:

- pos. 1 is between blocks 1 and 2 of the inner layer
- pos. 2 is between blocks 2 and 3 of the inner layer
- pos. 3 is between blocks 3 and 4 of the inner layer
- pos. 4 is between blocks 1 and 2 of the outer layer
- pos. 5 is between blocks 2 and 3 of the inner layer

All wedges, in the 5 positions, have the same cross section surface (the one of the smallest wedge in the design: 122.8mm²).

The reference radius for the multipole calculation is 10 mm.

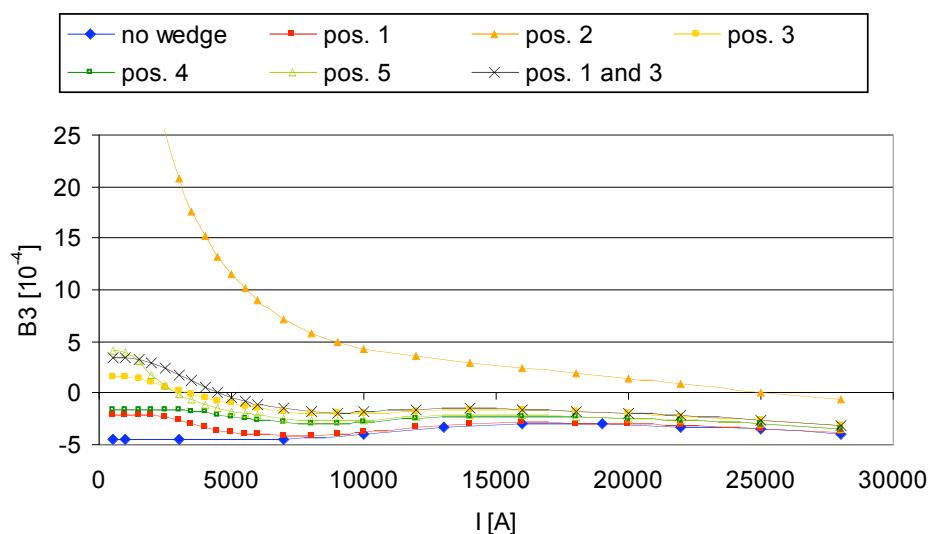


Fig. 52. Variation of b_3 as a function of the iron wedge position

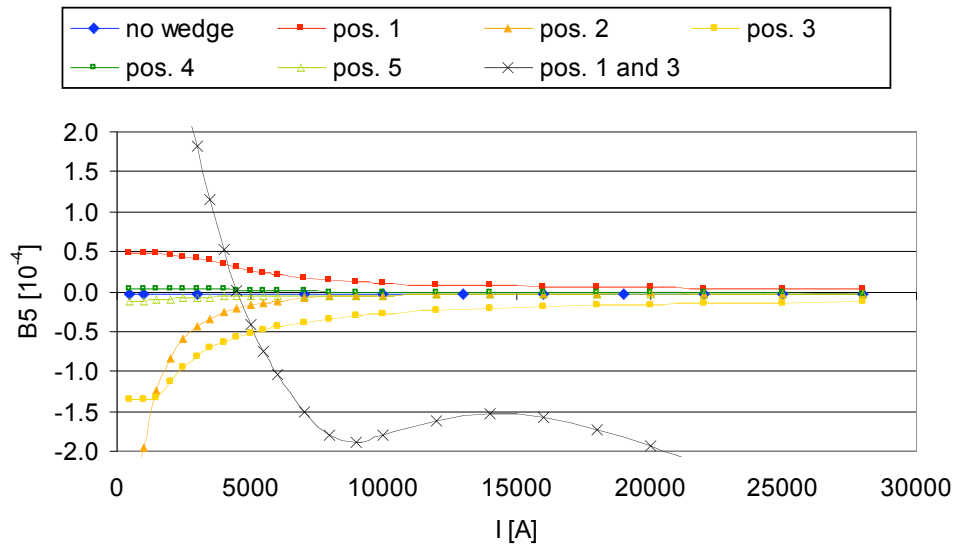


Fig. 53. Variation of b_5 as a function of the iron wedge position

It is also possible to modulate the influence of the iron wedge by changing its surface as shown below for the b_3 variation (Fig.54):

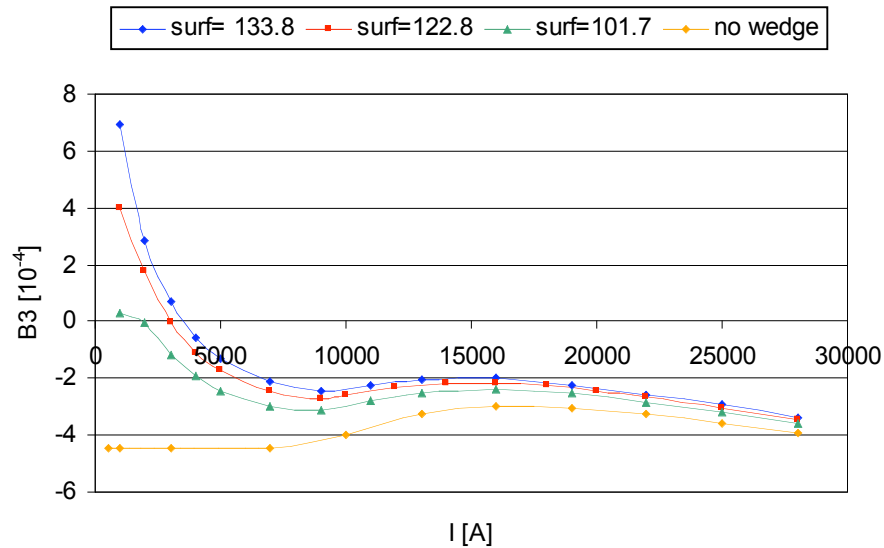


Fig. 54. Variation of b_3 as a function of the iron wedge surface (iron wedge in pos. 5)

(The surfaces are given in mm^2)

8. CONCLUSIONS

8.1 The preliminary magnet designs, made for 2 types of magnet concept, have shown that a Nb₃Sn strand of 1.25 mm Φ and a copper to non-copper of 1.25 was suitable to reach 15 T on the conductor in high field and large bore dipoles, if a critical current density of 1500 A/mm² in the non-copper part is obtained at 15 T and 4.2 K.

8.2 At 4.2 K, the bore field obtained in the 2 types of magnet concept is around 14 T for 15 T quenching on the conductor. To reach 15 T, at 4.2 K in the bore field, the critical current density should be increased by 10 %. At 1.9 K, the bore fields can attain 15 T.

8.3 In the layer design, the fields are around 14.3 T with a 26 mm wide cable for the 3 studied apertures of 88, 130, 160 mm. The layer design magnet is limited for apertures larger than 88 mm by the high transversal pressures (150-200 MPa) on the cable leading to a supplementary current degradation of the cable in brittle materials. The mechanical design of the layer structure foresees a pre-stress of the coils before energization. The value of the pre-stress depends on the coil mechanical characteristics (Apparent Young's modulus, differential contraction).

8.4 In the slot design, the field values calculated are around 13.9 T with cable width of 15.6 and 20.8 mm. The slot design uses rectangular cables and presents smaller pressures on the cables. This design seems more adapted to large bore dipoles. Opposed to the layer design, which is limited vertically in the number of conductors, the slot design has no lateral limitation. But the conductors are more distant from the bore and the design has a less efficient transfer function. The self-inductance can be modulated by the choice of the height of the cable.

The mid-plane is free of conductors on a 4 mm gap. The temperature margin of the cable close to the mid-plane is larger in the layer design. These characteristics are interesting since the beam losses have a major horizontal distribution.

It has been shown that the multipole contents can be controlled in the slot design by an appropriate choice of the notch angle or by inserting inert conductors (spacers) in the slots. The sc cable losses are lower due to a field distribution more parallel to the cable broad face.

Due to the cable hard bend in the coil ends, the coil winding stays a challenge and would need R&D.

8.5 For the NED dipole having an aperture of 88 mm, the layer design is then more appropriate.

8.6 It has been shown in the present report that the high magnetisation of the filaments leading to high multipole content up to 2 T can be compensated by the insertion of ferromagnetic material in the magnet design. The average filament size of 50 μ m can be accepted in the strand specification from the multipole point of view.

REFERENCES

- [1] CARE ref : <http://esgard.lal.in2p3.fr/Project/Activities/current/CARE>
- [2] “High Field Accelerator Magnet R&D in Europe”
A. Devred, D.E. Baynham, L. Bottura, M. Chorowski, P. Fabbriatore, D. Leroy, A. den Ouden, J.M. Rifflet, L. Rossi, O. Vincent-Viry and G. Volpini
IEEE Trans. Appl. Supercond., Vol.14 No.2, pp.339-344, 2004.
- [3] “The USA experience on Nb₃Sn and Bi-based superconductors and future plans”
R. Scanlan
HHH-AMT WAMS (Workshop on Accelerator Magnet Superconductors), 22-24 March 2004, Archamps, France.
<http://amt.web.cern.ch/amt/activities/workshops/WAMS2004/>
- [4] “Design and Manufacture of a Large Bore 10 T Superconducting Dipole for the CERN Cable Test Facility”
D. Leroy, G. Spigo, A. Verweij, H. Boschmann, R. Dubbeldam, J. Gonzalez-Pelayo
IEEE Trans. Appl. Supercond., Vol 10, No.1. pp178, March 2000.
- [5] “Construction of a 56 mm Aperture High-Field Twin-Aperture Superconducting Dipole Model Magnet for the LHC”
J. Ahlbaeck, D. Leroy, L. Oberli, D. Perini, J. Salminen, M. Savalainen, J. Soini, G. Spigo
IEEE transactions on Magnetics, Vol.32, No 4, pp.2097, July 1996.
- “Design Features and Performances of a 10 T Twin Aperture Model Dipole for LHC”
D. Leroy, L. Oberli, D. Perini, A. Siemko, G. Spigo
Proceedings of the 15 th International Conference on Magnet Technology, Beijing, China (1997), Science Press.
- [6] “ROXIE: Routine for the optimization of magnet X-sections, inverse field calculation and coil end design”
S. Russenschuck
Proceedings of the first international Roxie users meeting and workshop, 16-18 March 1998, CERN, Switzerland
- [7] “2D Magnetic induction analytical calculation”
O. Vincent-Viry
CERN/AT/MAS Internal Note 2003-10, November 2003
- [8] “Electrodynamics of superconducting cables in accelerator magnets”
A. P. Verweij
PHD Thesis, Twente University, The Netherlands, 1995
- [9] *G.Spigo Private communication*
- [10] “Characterization of the Thermo-Mechanical Behaviour of Insulated Cable Stacks representative of Accelerator Magnet Coils”
M. Reyrier, A. Devred, M. Durante, C. Gourdin, P. Vedrine
IEEE Trans. Appl. Supercond., Vol.11 No. 1, pp.3066-3069, 2001

- [11] “First Results of Slot Dipole at Saclay
A. Patoux, J. Perot
III International ICFA Workshop, Protvino, USSR (1981)
- [12] “Test of New Accelerator Superconducting Dipole suitable for high Precision Field”
A.Patoux, J.Perot, J.M.Rifflet
IEEE Transaction on Nuclear Science, Vol. NS-30, No 4, August 1983, pp3681.

9. ANNEX I

Fit for the critical current density J_c of Nb_3Sn as a function of field B , temperature T and stress ϵ

$$J_c(B, T, \epsilon) = \frac{C_{Nb_3Sn}(\epsilon)}{\sqrt{B}} \left[1 - \frac{B}{B_{C2}(T, \epsilon)} \right]^2 \left[1 - \left(\frac{T}{T_{C0}(\epsilon)} \right)^2 \right]^2$$

$$C_{Nb_3Sn}(\epsilon) = C_{Nb_3Sn,0} (1 - \alpha_{Nb_3Sn} |\epsilon|^{1.7})^{0.5}$$

$$\frac{B_{C2}(T, \epsilon)}{B_{C20}(\epsilon)} = \left[1 - \left(\frac{T}{T_{C0}(\epsilon)} \right)^2 \right] \left\{ 1 - 0.31 \left[\frac{T}{T_{C0}(\epsilon)} \right]^2 \left[1 - 1.77 \ln \left(\frac{T}{T_{C0}(\epsilon)} \right) \right] \right\}$$

$$B_{C20}(\epsilon) = B_{C20m} \left(1 - \alpha_{Nb_3Sn} |\epsilon|^{1.7} \right)$$

$$T_{C0}(\epsilon) = T_{C0m} \left(1 - \alpha_{Nb_3Sn} |\epsilon|^{1.7} \right)^3$$

$$\alpha_{Nb_3Sn} = \begin{cases} = 900 & \text{for compressive stress } (\epsilon < 0) \\ = 1250 & \text{for tensile stress} \end{cases}$$

B_{C20m} is the secondary critical induction at 0K and no stress

$$B_{C20m} = \begin{cases} = 24T & \text{for binary compounds} \\ = 28T & \text{for ternary compounds} \end{cases}$$

T_{C0m} is the critical temperature at 0T and no stress

$$T_{C0m} = \begin{cases} = 16K & \text{for binary compounds} \\ = 18K & \text{for ternary compounds} \end{cases}$$

C_{Nb_3Sn} is an interpolation factor

For example $C_{Nb_3Sn} = 48000 \text{ A} \cdot \text{T}^{0.5} \cdot \text{mm}^{-2}$ for $J_c = 3000 \text{ A/mm}^2$ at 12T, 4.2K

Reference:

“Supraconducteurs à basse température critique pour électro-aimants”

A.Devred

Rapport CEA –R-6011

CEA Saclay

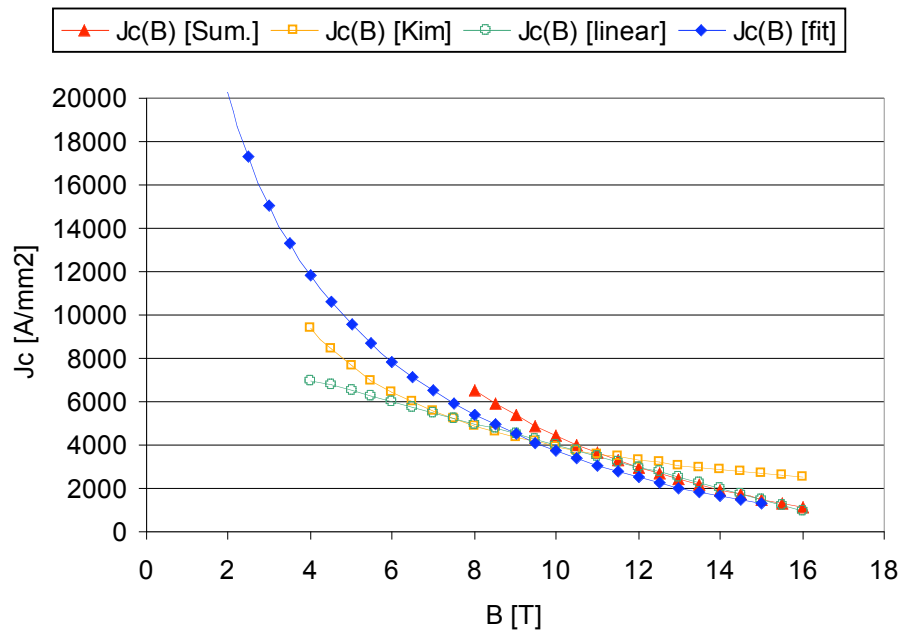


Fig. I-1 Comparison of various fits for the Nb₃Sn critical current density (for a ternary compound under a tensile deformation of 0.003)

Jc [Sum.] is the Summers' parameterisation
 Jc [Kim] is the Kim parameterisation
 Jc [linear] is a linear approximation
 Jc [fit] is the fit used for losses calculation in this report.

10. ANNEX II

88 mm layer dipole with 2 types of cables

II.1.Cables characteristics:

cable name	strand diam. [mm]	strand number	Cu/non_Cu	height [mm]	width inner [mm]	width outer [mm]	insul. [mm]	Jc_str at 15T, 4.2K [A/mm ²]	Jc_cab at 15T, 4.2K [A/mm ²]
CK1_i	1.35	34	1.25	23.868	2.349	2.565	0.2	666.67	421.2
CK1_o	1.15	40	1.8	23.92	2.001	2.185	0.2	535.71	330.4

The iron yoke thickness is 300 mm.

II.2.Magnetic aspects:

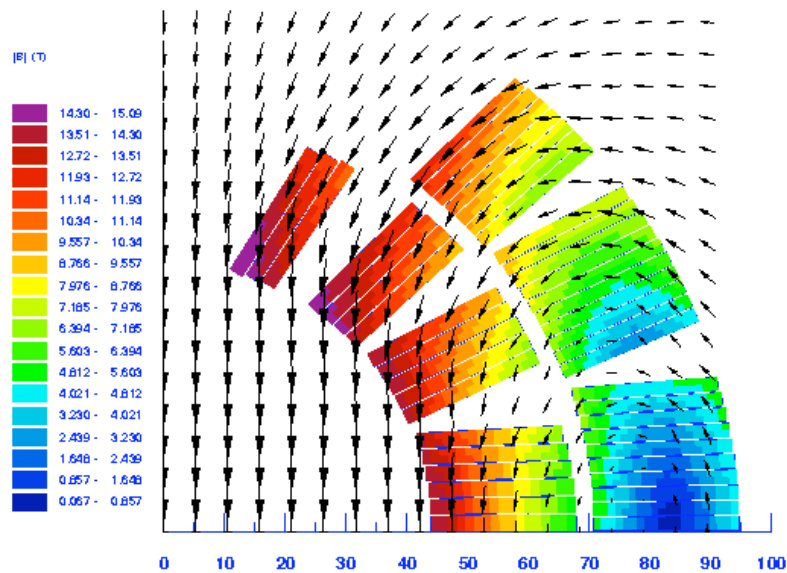


Fig. II-1 Magnetic induction distribution (design CK1)

central field [T]	I [A]	b1	b3	b5	b7	L [mH/m]	E/m [kJ/m]	copper current density (i / o) [A/mm ²]
14.45	28230	-	-2.68	0.02	0.008	4.45	1772.8	1044.1 / 1056.9

The reference radius for the multipole calculation is 10 mm.

This structure has not been optimized to decrease the multipole components levels.

Block number	Peak field [T]	% on load line [%]	Peak/Central [%]
1	14.26	95.3	98.7
2	14.28	95.4	98.9
3	14.76	98.1	102.2
4	15.09	100.0	104.5
5	6.63	59.0	45.9
6	9.24	74.2	64.6
7	12.45	91.8	86.2

II.3.Mechanical aspects:

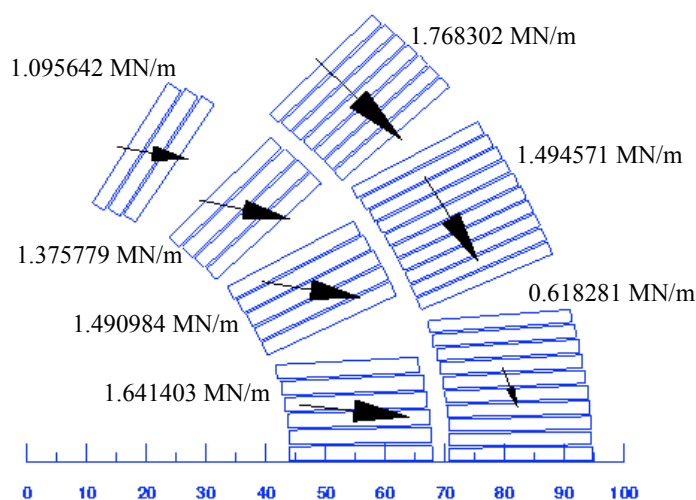


Fig. II-2 Magnetic forces distribution (design CK1) -(Only the 3rd digit is significant).

P_inner [MPa]	P_outer [MPa]	P_1 [MPa]	Sum Fx [MN/m]
-154.20	-161.68	105.51	15.66

Block	1	2	3	4	5	6	7
P_perp [MPa]	7.64	35.05	46.85	42.12	24.26	61.64	73.56

11. ANNEX III

Parametric study for a slot design dipole of 88 mm aperture, with finite iron yoke

III.1.Cable design:

The critical current density of the Nb₃Sn used is assumed to be 1500 A/mm² at 15T, 3000 A/mm² at 12T, at 4.2K.

The strand diameter is 1.25 mm and the copper to non-copper ratio is 1.25.

The insulation thickness is 0.2 mm.

The geometrical dimensions of cables are taken as following to insure a good mechanical stability [2]:

$$height = 1.04 \frac{nbr_str}{2} \phi_{str}$$

$$width = 2 * 0.87 \phi_{str}$$

where ϕ_{str} is the strand diameter and nbr_str the number of strands in the cable.

The cable used here is CR2, its cable critical current density is assumed to have a 10% degradation due to cabling.

III.2.Variation of the number of conductors in the design:

The aperture of the magnet is 88 mm, the iron yoke is finite and made of iron with Ms = 2.11T, its thickness is 350mm.

The number of notches is 3.

The numbers of conductors in each notch of a design are correlated to approach an elliptic overall shape. For all cases considered in this section, the ratio b/a of the ellipse is 0.777.

name	block 1 ncond	block 2 ncond	block 3 ncond	ncond total	iron yoke internal radius [mm]
-	-	-	-	-	
CRT2_311	11	6	2	19	100
CRT2_312	18	11	5	34	116
CRT2_313	25	16	8	49	134
CRT2_314	32	21	11	64	152
CRT2_315	40	26	14	80	172

name	central field [T]	I [A]	b3 [10 ⁻⁴]	b5 [10 ⁻⁴]	b7 [10 ⁻⁴]	L [mH/m]	E/m [kJ/m]	copper current density [A/mm ²]
CRT2_311	10.00	34100	11.9522	-0.9311	-0.0306	0.94	547.14	2500.85
CRT2_312	11.40	25345	-25.1015	-0.1920	-0.0223	2.65	852.18	1858.77
CRT2_313	12.04	20885	-37.6458	0.0583	-0.0182	5.12	1116.91	1531.68
CRT2_314	12.47	18275	-42.7717	0.1591	-0.0157	8.29	1383.99	1340.26
CRT2_315	12.81	16470	-44.4571	0.2011	-0.0139	12.42	1684.05	1207.89

notch 1					
name	P+	P-	P -azi	Sum Fx	F_notch
-	[MPa]	[MPa]	[MPa]	[MN/m]	[MN/m]
CRT2_311	90.12	-20.59	-30.52	2.18	0.904
CRT2_312	110.84	-20.11	-22.37	2.81	1.179
CRT2_313	125.31	-18.97	-17.89	3.27	1.382
CRT2_314	138.82	-18.16	-15.25	3.68	1.569
CRT2_315	153.45	-18.02	-13.49	4.12	1.761

notch 2					
name	P+	P-	P -azi	Sum Fx	F_notch
-	[MPa]	[MPa]	[MPa]	[MN/m]	[MN/m]
CRT2_311	45.36	-5.65	-47.79	2.52	0.516
CRT2_312	65.16	-9.10	-40.32	3.54	0.729
CRT2_313	79.71	-9.94	-34.24	4.23	0.907
CRT2_314	91.96	-10.35	-30.23	4.83	1.061
CRT2_315	103.29	-10.23	-26.70	5.39	1.210

notch 3					
name	P+	P-	P -azi	Sum Fx	F_notch
-	[MPa]	[MPa]	[MPa]	[MN/m]	[MN/m]
CRT2_311	8.80	0.00	-20.82	1.17	0.114
CRT2_312	20.62	-1.72	-26.80	2.47	0.246
CRT2_313	31.15	-2.06	-26.48	3.41	0.378
CRT2_314	38.71	-2.79	-25.37	4.19	0.467
CRT2_315	45.80	-2.82	-23.52	4.86	0.559

12. ANNEX IV

Parametric study for a slot design dipole of 88 mm aperture, with infinite iron yoke of infinite permeability

IV.1.Cable designs:

The critical current density of the Nb₃Sn used is assumed to be 1500 A/mm² at 15T, 3000 A/mm² at 12T, at 4.2K.

The strand diameter is 1.25 mm and the copper to non-copper ratio is 1.25.

The insulation thickness is 0.2 mm.

The geometrical dimensions of cables are taken as following to insure a good mechanical stability [2]:

$$height = 1.04 \frac{nbr_str}{2} \phi_{str}$$

$$width = 2 * 0.87 \phi_{str}$$

where ϕ_{str} is the strand diameter and nbr_str the number of strands in the cable.

Here the degradation of the cable critical current density due to cabling is taken as 0%.

The different cables designs investigated are:

name	strand number	height [mm]	width [mm]	Jc (cable + insul.) at 4.2K, 15T [A/mm ²]
CR2	20	13	2.175	474.21
CR3	22	14.3	2.175	475.50
CR4	24	15.6	2.175	476.58

IV.2.Parametrical study:

The magnet structures investigated in this section are of block-motor type, with 3 notches.

The iron yoke is modelled as infinite and of infinite permeability.

IV.2.1.Impact of notch angle:

Notch 1 is the one closer to the mid-plane of the magnet.

The numbers of conductors in blocks are respectively 33, 25 and 15 for notches 1,2 and 3. The cable used is CR2.

IV.2.1.1. Notch 1:

Angles for notches 2 and 3 are respectively 40 and 60 degrees, we then get:

notch 1 angle [deg] / [%]	central field [T] / [%]	b3 [10 ⁻⁴] / [%]	b5 [10 ⁻⁴] / [%]	b7 [10 ⁻⁴] / [%]	inductance [mH/m] / [%]	stored energy [kJ/m] / [%]
10	-13.22	-139.13	6.89	4.89	11.56	1574.01
+50	-1.13	41.83	-212.70	-59.48	-4.07	-4.76
+100	-2.78	97.82	-458.53	-110.72	-2.22	-2.46

notch 1 angle [deg] / [%]	P+ (1) [MPa] / [%]	P- (1) [MPa] / [%]	P-azi (1) [MPa] / [%]	P+ (2) [MPa] / [%]	P- (2) [MPa] / [%]	P-azi (2) [MPa] / [%]	P+ (3) [MPa] / [%]	P- (3) [MPa] / [%]	P-azi (3) [MPa] / [%]
10	163.84	-6.09	-13.63	102.39	-8.23	-38.70	57.86	-2.66	-67.53
+50	-10.72	54.38	-7.33	1.59	1.63	0.98	2.12	-4.35	0.14
+100	-15.87	72.21	-25.09	3.82	3.96	2.33	0.92	-1.74	0.12

IV.2.1.2. Notch 2:

Angles for notches 1 and 3 are respectively 10 and 60 degrees, we then get:

notch 2 angle [deg] / [%]	B1 [T] / [%]	b3 [10 ⁻⁴] / [%]	b5 [10 ⁻⁴] / [%]	b7 [10 ⁻⁴] / [%]	inductance [mH/m] / [%]	stored energy [kJ/m] / [%]
30	-13.95	24.86	9.25	-0.15	12.57	1752.79
+16.67	-2.40	-334.02	-49.46	-1364.31	-4.11	-5.14
+33.33	-5.21	-659.58	-25.48	-3272.34	-8.01	-10.20

notch 2 angle [deg] / [%]	P+ (1) [MPa] / [%]	P- (1) [MPa] / [%]	P-azi (1) [MPa] / [%]	P+ (2) [MPa] / [%]	P- (2) [MPa] / [%]	P-azi (2) [MPa] / [%]	P+ (3) [MPa] / [%]	P- (3) [MPa] / [%]	P-azi (3) [MPa] / [%]
30	167.76	-11.79	-14.95	127.67	-6.64	-44.25	55.14	-2.60	-66.86
+16.67	-3.36	-12.30	2.00	-10.12	6.37	-6.51	2.08	1.21	0.43
+33.33	-2.34	-48.33	-8.81	-19.80	23.88	-12.55	4.92	2.19	1.01

IV.2.1.3. Notch 3:

Angles for notches 1 and 2 are respectively 10 and 30 degrees, we then get:

notch 3 angle [deg] / [%]	b1 [T] / [%]	b3 [10 ⁻⁴] / [%]	b5 [10 ⁻⁴] / [%]	b7 [10 ⁻⁴] / [%]	inductance [mH/m] / [%]	stored energy [kJ/m] / [%]
50	-13.94	58.59	-18.47	1.98	13.39	1725.21
+10	0.94	-43.08	-75.10	-15.88	-3.11	2.39
+20	0.10	-57.57	-150.10	-107.78	-6.16	1.60

notch 3 angle [deg] / [%]	P+ (1) [MPa] / [%]	P- (1) [MPa] / [%]	P-azi (1) [MPa] / [%]	P+ (2) [MPa] / [%]	P- (2) [MPa] / [%]	P-azi (2) [MPa] / [%]	P+ (3) [MPa] / [%]	P- (3) [MPa] / [%]	P-azi (3) [MPa] / [%]
50	156.02	-11.18	-13.59	119.01	-6.88	-39.60	68.22	-1.51	-64.59
+10	5.37	4.07	6.58	5.49	-1.05	7.59	-8.39	38.19	2.96
+20	7.53	5.47	9.96	7.27	-3.37	11.76	-19.17	72.27	3.51

IV.2.2. Impact of notch length:

The varying parameter is now the number of conductors in each notch. Notches angles are kept constant and are respectively 10, 30 and 50 degrees for notches 1, 2 and 3.

The cable used is CR2.

IV.2.2.1. Notch 1:

The number of conductors in notches 1 and 2 are 25 and 15.

notch 1 conductor number - / [%]	Central field [T] / [%]	b3 [10 ⁻⁴] / [%]	b5 [10 ⁻⁴] / [%]	b7 [10 ⁻⁴] / [%]	inductance [mH/m] / [%]	stored energy [kJ/m] / [%]
28	-13.83	51.28	-19.17	2.03	11.80	1579.63
+17.86	0.79	14.25	-3.65	-2.53	13.48	9.22
+35.71	1.45	23.13	-6.61	-4.92	27.92	18.56
+53.57	2.05	28.67	-9.13	-7.13	43.32	28.15

The inner radius of the iron yoke is determined by the length of the longer notch, which here is always notch1. The inner radiuses of the iron yoke are, for the 4 previous cases, respectively 140, 153, 166 and 179 mm.

notch 1 conductor number	P+ (1) [MPa] - / [%]	P- (1) [MPa] / [%]	P-azi (1) [MPa] / [%]	P+ (2) [MPa] / [%]	P- (2) [MPa] / [%]	P-azi (2) [MPa] / [%]	P+ (3) [MPa] / [%]	P- (3) [MPa] / [%]	P-azi (3) [MPa] / [%]
28	144.47	-9.02	-12.85	116.80	-7.98	-38.61	68.73	-1.73	-65.06
+17.86	8.00	23.93	5.77	1.89	-13.83	2.55	-0.74	-12.82	-0.72
+35.71	15.49	37.86	9.58	3.85	-27.77	3.82	-1.08	-30.59	-1.60
+53.57	23.10	42.18	11.94	5.72	-43.24	4.35	0.08	-48.09	-2.52

IV.2.2.2. Notch 2:

notch 2 conductor number	central field	b3 [10 ⁻⁴] / [%]	b5 [10 ⁻⁴] / [%]	b7 [10 ⁻⁴] / [%]	Inductance [mH/m] / [%]	Stored energy [kJ/m] / [%]
22	-13.83	60.63	-18.79	2.06	12.28	1667.34
+13.64	0.77	-3.36	-1.71	-3.89	9.09	3.47
+27.27	1.48	-6.42	-3.68	-7.26	18.68	7.03
+40.91	2.17	-9.25	-5.76	-10.26	28.80	10.73

The inner radius of the iron yoke is 153 mm.

notch 2 conductor number	P+ (1) [MPa] / [%]	P- (1) [MPa] / [%]	P-azi (1) [MPa] / [%]	P+ (2) [MPa] / [%]	P- (2) [MPa] / [%]	P-azi (2) [MPa] / [%]	P+ (3) [MPa] / [%]	P- (3) [MPa] / [%]	P-azi (3) [MPa] / [%]
22	153.30	-12.41	-14.55	112.31	-5.91	-41.06	67.26	-2.28	-65.43
+13.64	1.78	-9.94	-6.60	5.96	16.36	-3.57	1.42	-33.87	-1.28
+27.27	3.79	-20.61	-12.23	11.48	32.37	-7.13	3.92	-62.05	-2.65
+40.91	6.14	-33.70	-16.95	17.69	33.29	-10.56	5.33	-77.55	-4.00

IV.2.2.3. Notch 3:

notch 3 conductor number	central field	b3 [10 ⁻⁴] / [%]	b5 [10 ⁻⁴] / [%]	b7 [10 ⁻⁴] / [%]	Inductance [mH/m] / [%]	Stored energy [kJ/m] / [%]
12	-13.90	80.67	-18.51	1.95	12.62	1713.90
+25.00	0.25	-27.37	-0.21	1.71	6.13	0.66
+50.00	0.52	-47.60	-1.22	1.34	12.62	1.82
+75.00	0.90	-63.02	-2.62	0.09	19.44	3.49

The inner radius of the iron yoke is 153 mm.

notch 3 conductor number	P+ (1) [MPa] / [%]	P- (1) [MPa] / [%]	P-azi (1) [MPa] / [%]	P+ (2) [MPa] / [%]	P- (2) [MPa] / [%]	P-azi (2) [MPa] / [%]	P+ (3) [MPa] / [%]	P- (3) [MPa] / [%]	P-azi (3) [MPa] / [%]
12	160.84	-11.94	-14.48	120.69	-7.15	-42.47	60.62	-0.32	-68.54
+25.00	-2.99	-6.37	-6.16	-1.39	-3.79	-6.76	12.53	376.25	-5.75
+50.00	-5.25	-11.04	-11.47	-1.91	-2.60	-12.44	23.44	892.54	-10.99
+75.00	-6.51	-16.88	-15.99	-1.39	-8.85	-17.08	33.42	1437.7	-15.64

IV.2.3. Impact of notch width:

The numbers of conductors in blocks are respectively 33, 25 and 15 for notches 1, 2 and 3. The notches angles are respectively 10, 35 and 65 degrees.

The only varying parameter is the cable height: cables CR2, 3 and 4 are compared.

cable height [mm] / [%]	strand number	central field [T] / [%]	b3 [10 ⁻⁴] / [%]	b5 [10 ⁻⁴] / [%]	b7 [10 ⁻⁴] / [%]	inductance [mH/m] / [%]	stored energy [kJ/m] / [%]
13.00	20	-13.61	-58.18	4.68	1.95	12.05	1662.64
+10	22	2.05	-0.87	-1.60	-3.15	-0.15	4.10
+20	24	3.92	-1.80	-3.31	-6.49	-0.29	7.92

cable height [mm] / [%]	P+ (1) [MPa] / [%]	P- (1) [MPa] / [%]	P-azi (1) [MPa] / [%]	P+ (2) [MPa] / [%]	P- (2) [MPa] / [%]	P-azi (2) [MPa] / [%]	P+ (3) [MPa] / [%]	P- (3) [MPa] / [%]	P-azi (3) [MPa] / [%]
13.00	162.12	-10.34	-15.24	114.74	-7.07	-41.37	56.29	-2.63	-67.15
+10	-5.55	-5.88	4.33	-5.73	-5.54	4.29	-5.60	-11.77	4.33
+20	-10.36	-12.81	8.39	-10.58	-13.43	8.29	-10.51	-21.87	8.38

13. ANNEX V

Parametric study for a slot design dipole of 160 mm aperture, with finite iron yokeV.1.Variation of the number of notches:

The cable used here is CR2 (with 10% critical current degradation due to cabling).

The aperture of the magnet is 160 mm and the iron yoke thickness is 640mm

The total number of conductors is the same for all designs (77 conductors).

name	notches number	ncond	block angle [deg]	iron yoke internal radius [mm]
-	-	-		
CRT2_321	3	37, 26, 14	10, 32.5, 55	200
CRT2_322	4	26, 22, 27, 12	10, 25, 10, 55	172
CRT2_323	5	22, 19, 16, 12, 8	10, 22.5, 35, 47.5, 60	162

name	Main [T]	I [A]	b3 [10^{-4}]	b5 [10^{-4}]	b7 [10^{-4}]	L [mH/m]	E/m [kJ/m]	copper current density [A/mm^2]
-								
CRT2_321	11.90	20575	4.7826	-0.0585	0.0016	15.27	3232.24	1508.94
CRT2_322	12.08	19310	2.3633	-0.1860	0.0010	15.31	2853.61	1416.17
CRT2_323	12.29	19155	-1.8473	-0.1887	0.0006	15.02	2756.03	1404.80

name	P+ max [MPa]	P- max [MPa]	P -azi max [MPa]	Sum Fx total [MN/m]	F_notch max [MN/m]
-					
CRT2_321	205.51	-29.95	-35.11	16.68	2.282302
CRT2_322	134.33	-22.05	-37.38	16.18	1.459580
CRT2_323	111.74	-20.14	-37.12	16.53	1.190832

F_notch max is the maximum force obtained in any notch of the structure.

V.2.Variation of cable height:

The aperture of the magnet is 160 mm and the iron yoke thickness is 640mm.
The magnets have all 3 notches of angles 12, 34 and 56 degrees.

The cable used here are CR2, CR5, CR6. They use the same strand.
The total amount of strands is the same in all the designs (1560 strands).

name	cable name	strand number	cable height [mm]	cable width [mm]	iron yoke internal radius [mm]
-	-	-			
CRT2_341	CR2	20	13	2.175	200
CRT5_342	CR5	30	19.5	2.175	172
CRT6_343	CR6	40	26	2.175	160

name	central field [T]	I [A]	b3 [10 ⁻⁴]	b5 [10 ⁻⁴]	b7 [10 ⁻⁴]	L [mH/m]	E/m [kJ/m]	copper current density [A/mm ²]
-								
CRT2_341	-11.77	20390	-0.3771	-0.0884	0.0012	15.12	3143.40	1495.37
CRT5_342	-12.28	28805	4.8272	-0.1016	0.0011	7.11	2950.32	1408.35
CRT6_343	-13.00	38350	13.2493	-0.1120	0.0006	4.22	3103.81	1406.27

notch 1					
name	P+ [MPa]	P- [MPa]	P -azi [MPa]	Sum Fx [MN/m]	F_notch [MN/m]
-					
CRT2_341	196.72	-28.05	-17.09	4.97	2.193
CRT5_342	140.90	-26.33	-28.25	5.17	2.234
CRT6_343	122.39	-27.07	-44.17	5.87	2.478

notch 2					
name	P+ [MPa]	P- [MPa]	P -azi [MPa]	Sum Fx [MN/m]	F_notch [MN/m]
-					
CRT2_341	134.69	-18.31	-33.99	6.13	1.513
CRT5_342	89.42	-12.81	-51.08	6.30	1.494
CRT6_343	72.37	-9.84	-75.72	7.28	1.626

notch 3					
name	P+ [MPa]	P- [MPa]	P -azi [MPa]	Sum Fx [MN/m]	F_notch [MN/m]
-					
CRT2_341	65.83	-6.54	-30.02	5.61	0.771
CRT5_342	36.62	-3.27	-39.04	5.08	0.650
CRT6_343	19.15	-0.27	-39.35	4.14	0.491